CONTENTS

Ultrasonic Continuous-Wave Beam-Power Measurements; International Intercomparison

Carl E. Tschiegg,* Martin Greenspan,** and Donald G. Eitzen*

National Bureau of Standards, Washington, DC 20234

October 26, 1982

Some quartz transducers designed and fabricated at the National Bureau of Standards as transmitters of ultrasonic power appear to be sufficiently stable and linear to serve as standards. Therefore, an international intercomparison of measurements of the continuous-wave (cw) power emitted by these standards was arranged. Each of the seven participating laboratories performed such measurements using one or more methods representing its practice and reported the results to the National Bureau of Standards which served as the pilot laboratory. We present the results mostly in the form of tables. Some remarks on stability are appended.

Key words: intercomparison of standards; ultrasonic power standards; ultrasonic transducers.

1. Introduction

In 1974, Thomas L. Zapf, [1][1] of the then Electromagnetics Division of the National Bureau of Standards in Boulder, CO, U.S.A., described a method for the measurement of the radiation conductance of an ultrasonic transducer by means of high-accuracy impedance measurements made with a twin-T null circuit. Also described were some quartz transducers designed and constructed so that they could be expected to be stable over long intervals of time. By the spring of 1975, Helmut M. Altschuler of the Electromagnetics Division of NBS Boulder was actively arranging the international comparison of ultrasonic beam-power measurements utilizing the new standards; the technical direction of the project was to be Zapf's responsibility. In the fall of 1976, when many of the arrangements with the participating laboratories had been completed, the responsibility for the project was transferred to Donald G. Eitzen, chief of the then Ultrasonic Standards Program Team in Washington, as a result of a management decision to consolidate some of the work in ultrasonics at NBS. Also transferred, besides some equipment, were 14 quartz transducers, having operating frequencies of

2, 3, 5, 10, and 15 MHz. These were calibrated by the modulated radiation-pressure method [2] over the ranges of ultrasonic power output from 1 to 8 mW up to 1 to 528 mW, and the transducers were found to be linear (i.e., power output proportional to square of voltage), so that each transducer could be characterized by a single radiation conductance (G_r). Furthermore, this G_r proved to be the same, within the estimated experimental errors, as that determined at very low power by the twin-T null method. Other transducers were also calibrated by a calorimetric method, using an instrument designed and built by Zapf et al. [3] at NBS Boulder and modified at NBS Washington[2]. Each transducer was calibrated (twice) at only one power level which varied, from case to case, over the range 50 to 750 mW. Again, the values of G_r agreed, within the estimated uncertainty, with those obtained by the other methods.

2. Procedure

Four ultrasonic transducers were selected for the intercomparison. They were intended to be operated at the fundamental series-resonance frequencies; these, together with the designations, follow:

---

*Mechanical Production Metrology Division, Center for Manufacturing Engineering, National Engineering Laboratory.
**Present address: 12 Granville Dr., Silver Spring, MD 20901.
[1]Figures in brackets denote literature references at the end of this paper.

---

[2]The modifications, which were rather extensive, were made by Franklin R. Breckenridge and Carl E. Tschiegg.

Standard No.	Operating Frequency	
	Nominal MHz	Actual MHz
3-16	2	1.995
3-18	2	1.995
3-20	5	5.046
3-22	5	5.015

The active element of each was a half-wave resonant, air-backed, x-cut quartz disc, having a "wrap-around" outer electrode to provide some electrostatic shielding. The discs were cut, polished, and plated (gold over chromium) by a commercial supplier. The transducers are shown in figure 1.
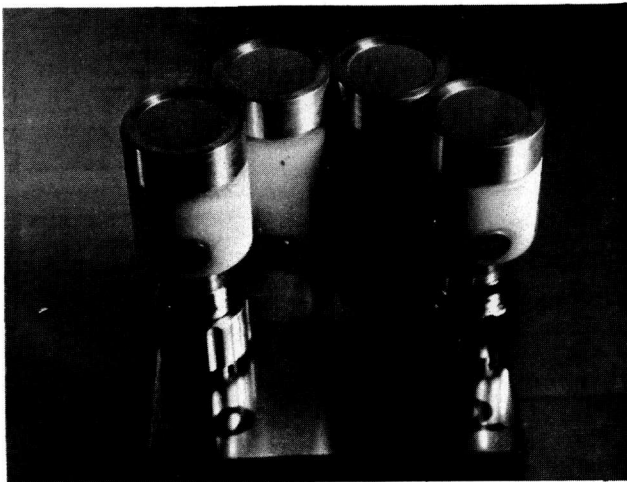
FIGURE 1. The four standard transducers.

The transducers were shipped to the participating laboratories and the measurements made in the following order:

1. National Bureau of Standards
   Boulder, CO, U.S.A.

2. National Bureau of Standards
   Washington, DC, U.S.A.

3. Radiation Protection Bureau
   Ottawa, Ontario, Canada

4. National Research Council
   Ottawa, Ontario, Canada

5. NBS (Remeasurement)

6. Bureau of Radiological Health
   Rockville, MD, U.S.A.

7. NBS (Remeasurement)

8. Ultrasonics Institute
   Sydney, Australia

9. NBS (Remeasurement)

10. Physikalisch-Technische Bundesanstaldt
    Braunschweig, FRG

11. NBS (Remeasurement)

12. National Physical Laboratory
    Teddington, Middlesex, U.K.

13. NBS (Remeasurement)

The instructions to the participating laboratories are reproduced in the Appendix. Each laboratory used its own method or methods, a total of eight. The methods are listed together with their code designations in table 1.

TABLE 1. *Methods of ultrasonic cw beam power measurement and codes.*

Method	Code
Radiation balance, direct	RD
Radiation balance, feedback	RF
Radiation balance, modulated	RM
Calorimeter	C
Optical (Raman-Nath)	O
Impedance, twin-T null	T
Impedance, Q-meter	Q
Reciprocity	R

The voltage levels and tolerances specified in the Appendix were selected to cover ultrasonic power levels roughly as follows:

low	2.5	—	25 mW
medium	25	—	250 mW
high	250	—	2500 mW

3. Results

The results are given in tables 2, 3, 4, and 5 for transducers 3-16, 18, 20, and 22, respectively. In the column headed "Code" the arabic numeral following the method designation (as in e.g., RD-1) denotes one of the participating laboratories. In cases in which a laboratory used several methods, the associated numeral is different for each method. Each laboratory was furnished a key that enabled it to identify its own work, but not that of others. An exception is the pilot laboratory, NBS, for which RM-1 and T-1 are used.

In these tables, U_v is the fractional uncertainty in the measurement of input voltage, and U_b is that in the radiation conductance, taking into account that in the voltage. See the Appendix for details. Each investigator, acting in accordance with instructions, estimated these uncertainties by his own methods, so that the several laboratories have not reported on a common basis.

Inspection of tables 2, 3, 4, and 5 reveals that by and large, there is rather remarkable agreement in the measurement of ultrasonic beam power at the power levels specified among the several laboratories and methods (or cases).[3] In order to see this better, it is convenient to look at the departure of each result from some sort of grand average of all results. The question is how to weight the individual averages of the radiation conductance $\overline{G}_r$, in the calculation of the grand average, $\overline{\overline{G}}_r$. Our first thought was to use weights inversely proportional to the estimated errors, but we discarded this because, as has been pointed out, the reported errors are not comparable. We eventually decided to use purely statistical weights, that is, weights equivalent to the reciprocal variances. However, it was easier to use an approximation to the variance calculated from the range (max-min in tables 2, 3, 4, and 5) and the mean value of the ratio of the range to the standard deviation (square root of the variance); this ratio depends on the number of data. Values of it are given in table 2.4.1 of Snedecor [4]. No deep significance is attached to the grand averages, $\overline{\overline{G}}_r$; we present them as being perhaps good enough for the present purpose. Data for which the ranges were not given were not used in the calculation of the grand average, nor were those averages used which were calculated from fewer than three data. The deviations from the grand average were given in table 6.

[3]Some of the methods used by the participating laboratories, e.g., steady radiation pressure and calorimetric, are in principal capable of measuring average pulsed power. In some applications, such as medical imaging, such average powers might be much lower than those used in these tests and the conclusion would not apply.

We can consolidate the material given in table 6 in the form of table 7, in which the number of cases where the absolute value of the deviation, $|(\overline{G}_r - \overline{\overline{G}}_r)/\overline{\overline{G}}_r|$ is less than various amounts (in percent). A method of measurement by a particular laboratory forms a case, and the results are presented separately for the two nominal frequencies; the values for transducers 3-16 and 3-18 are lumped in one column and those for 3-20 and 3-22 in the other. We see that at 2 MHz the deviations are less than 1 percent in 11 percent of the cases and less than 3 percent in 33 percent of the cases. For 5 MHz the peak is sharper; the values are 40 and 80 percent of the cases, respectively. At both frequencies, more than 90 percent of the cases have $\overline{G}_r$ within 9 percent of $\overline{\overline{G}}_r$ and if one case (RD-3) were ignored, the figure would be 100 percent.

We can only speculate as to why the data are better at 5 than at 2 MHz. Perhaps the increased absorption at 5 MHz eases the requirements on the anechoic materials, the performance of which is almost always less than one might hope.

It is worth noting that in each case except one (RD-3) the deviation (of the overall average for a case from the grand average) is less than the experimenter's estimate of the error. This would mean little if in most of the cases the results were all too high or all too low. But in consideration of the diversity of the methods employed, this is not likely, and it would seem that most of the experimenters have made conservative estimates of their errors.

The results are, on the whole, gratifying. They lead us to believe that one can really measure with acceptable accuracy the total cw sound power output of transducers in the frequency range 2-5 MHz and in the power range 2.5-2500 mW. Unfortunately, the same conclusion cannot be extended into the fractional milliwatt range that is important to applications (such as medical diagnosis) characterized by high peak but low average power. The prospects for extending agreement to microwatt levels of average power are probably good.

4. Stability

As shown in table 3 and its footnote n, one of the participants noticed a substantial change, between runs, of the value of G_r for transducer 3-18. Extensive measurements on this transducer were made upon its return to the pilot laboratory, but no significant changes from the pristine value were detected even after a three-day submersion of the operating face in water.

We have had a similar experience ourselves. A transducer of nominally identical construction as 3-18

TABLE 2. *Transfer standard No. 3-16 nominal frequency 2 MHz*.*

Code[a]	Power[b] Range	No. of Data	Applied Voltage			Radiation Conductance			
			Min	Max	U_V	Min	Max	Avg.	U_b
			V	V	±%	µS	µS	µS	±%
RD-1	low	5	30	30	0.25	9	12	11	22
	med	5	100	100	0.25	11.5	11.9	11.6	7
	high	5	180	180	0.25	12.0	12.2	12.1	5
	overall	15	30	180	—	9	12.2	11.54	—
RD-2	low	3	35	35	1.3	11.7	11.8	11.8	10
	med	12	56	71	1.3	11.2	11.9	11.5	10
	high	0	—	—	—	—	—	—	—
	overall	15	35	71	—	11.2	11.9	11.58	—
RD-3	low	10	30	30	0.5	24.9	38.5	29.9	?[c]
	med	10	100	100	0.5	10.4	12.6	10.9	7[c]
	high	10	180	180	0.5	11.5	12.6	12.00	2.8[c]
	overall	30	30	180	—	10.4	38.5	17.6[d]	—
RD-4	low	1	35[e]	35	2	9.3	9.3	9.3	19
	med	2	53	71	2[c]	10.8	11.7	11.2	19
	high	0	—	—	—	—	—	—	—
	overall	3	35	71	—	9.3	11.7	10.6	—
RF-1	low	6	26	26	0.2	10.6	11.2	10.9	6.1[c,f]
	med	6	81	82	0.2	10.9	11.2	11.0	5.6[c,f]
	high	7	254	259	1.0	11.1	11.8	11.4	7.6[c,f]
	overall	19	26	259	—	10.6	11.8	11.13	—
RF-3	low	3	35	35	1.3	11.7	11.8	11.7	10
	med	6	56	70	1.3	11.9	12.0	11.9	10
	high	0	—	—	—	—	—	—	—
	overall	9	35	70	—	11.7	12.0	11.86	—
RF-4	low	9/20[g]	26	36	0.3	10.3	11.2	10.9	3.8
	med	9/20	66	91	0.4	10.4	11.3	10.9	3.9
	high	9/20	146	187	0.5	10.5	11.2	10.9	4.2
	overall	27/60	26	187	—	10.3	11.3	10.87	—
RM-1	low	34	16	46	0.2	11.2	11.5	11.4	2.3
	med	15	66	135	0.2	11.3	11.3	11.3	2.3
	high	17	150	216	0.2	11.3	11.3	11.3	2.3
	overall	66	16	216	—	11.2	11.5	11.34	—
C-3[h]	i	i	i	i		i	i	11.1	7
C-5	low	3	35	36	1.3	11.3	12.3	11.8	10
	med	3	59	61	1.3	11.8	12.4	12.1	10
	high	0	—	—	—	—	—	—	—
	overall	6	35	61	—	11.3	12.4	11.94	—
0.1	low	0	—	—	—	—	—	—	—
	med	9	70	141	1.3	10.6	12.1	11.3	10
	high	5	176	211	1.3	10.9	11.7	11.3	10
	overall	14	70	211	—	10.6	12.1	11.29	—
Q-4	j	10	j	j	i	i	i	10.56	i
R-2[k]	low	6	30	38	i	10.9	11.5	11.1	17
	med	0	—	—	—	—	—	—	
	high	0	—	—	—	—	—	—	
	overall	6	30	38		10.9	11.5	11.1	
			weighted mean[p]					11.44	

*Footnotes follow table 5.

TABLE 3. *Transfer standard No. 3-18 nominal frequency 2 MHz**.

Code[a]	Power[b] Range	No. of Data	Applied Voltage			Radiation Conductance			
			Min V	Max V	U_V ±%	Min μS	Max μS	Avg. μS	U_b ±%
RD-1	low	5	30	30	0.25	8	10	9	22
	med	5	100	100	0.25	11.1	11.2	11.2	7
	high	5	180	180	0.25	11.7	11.9	11.8	5
	overall	15	30	180	—	8	11.9	10.66	—
RD-2	low	3	35	35	1.3	11.8	11.9	11.9	10
	med	12	56	71	1.3	11.2	11.8	11.5	10
	high	0	—	—	—	—	—	—	—
	overall	15	35	71	—	11.2	11.9	11.57	—
RD-3	low	10	30	30	0.5	16.3	43.0	31.4	35[c]
	med	10	100	101	0.5	12.6	14.0	13.2	6.7[c]
	high	10	180	180	0.5	11.2	11.5	11.3	3.0
	overall	30	30	180	—	11.2	43.0	18.64[m]	—
RD-4	low	1	35[e]	35	2.0	10.2	10.2	10.2	18
	med	2	53	71	1.9[c]	10.5	11.4	11.0	19[c]
	high	0	—	—	—	—	—	—	—
	overall	3	35	71	—	10.2	11.4	10.7	—
RF-1	low	7	25	26	0.2	10.0	10.8	10.4	5.5[c,f]
	med	7	81	82	0.2	10.0	10.7	10.3	5.6[c,f]
	high	7	254	256	1	10.5	11.1	10.7	7.6[c,f]
	overall	21	25	256	—	10.0	11.1	10.45	—
RF-3	low	3	35	35	1.3	11.0	11.3	11.2	10
	med	6	56	70	1.3	11.4	11.5	11.4	10
	high	0	—	—	—	—	—	—	—
	overall	9	35	70	—	11.0	11.5	11.35	—
RF4.1[n]	low	7/26[g]	21	36	0.3	11.2	12.5	11.7	3.8
	med	7/26	72	97	0.4	11.1	11.7	11.4	3.9
	high	6/22	160	296	0.5	11.8	12.2	11.9	4.2
	overall	20/74	21	296	—	11.1	12.5	11.65	—
RF4.2[n]	low	8/20[g]	22	32	0.3	10.3	11.0	10.7	3.8
	med	8/20	70	97	0.4	10.3	10.9	10.6	3.9
	high	8/20	140	191	0.5	10.4	10.9	10.7	4.2
	overall	24/60	22	191	—	10.3	11.0	10.65	—
RM-1	low	32	16	36	0.2	11.0	11.3	11.2	2.3
	med	13	46	150	0.2	11.0	11.2	11.1	2.3
	high	19	151	232	0.2	11.0	11.4	11.2	2.3
	overall	64	16	232	—	11.0	11.4	11.16	—
C-5	low	3	35	37	1.3	11.3	11.9	11.5	10
	med	3	56	58	1.3	10.9	12.2	11.5	10
	high	0	—	—	—	—	—	—	—
	overall	6	35	58	—	10.9	12.2	11.50	—
0-1	low	0	—	—	—	—	—	—	—
	med	9	70	141	1.3	10.8	11.9	11.4	10
	high	6	176	211	1.3	10.8	11.5	11.3	10
	overall	15	70	211	—	10.8	11.9	11.33	—
Q-4	j	10	j	j	i	i	i	10.24	i

95

Code[a]	Power[b] Range	No. of Data	Applied Voltage			Radiation Conductance			
			Min	Max	U_V	Min	Max	Avg.	U_b
			V	V	±%	μS	μS	μS	±%
R2.1[k,n]	low	2	30	40	i	10.6	10.9	10.7	17
	med	0	—	—	—	—	—	—	—
	high	0	—	—	—	—	—	—	—
	overall	2	30	40		10.6	10.9	10.7	
R2.2[k,n]	low	1	18	18	i	12.1	12.1	12.1	17
	med	0	—	—	—	—	—	—	—
	high	0	—	—	—	—	—	—	—
	overall	1	18	18		12.1	12.1	12.1	
			weighted mean[p]					11.12	

*Footnotes follow table 5.

TABLE 4. *Transfer standard No. 3-20 nominal frequency 5 MHz*.*

Code[a]	Power[b] Range	No. of Data	Applied Voltage			Radiation Conductance			
			Min	Max	U_V	Min	Max	Avg.	U_b
			V	V	±%	μS	μS	μS	±%
RD-1	low	5	12	12	0.25	49	67	58	22
	med	5	40	40	0.25	78	81	78	7
	high	5	100	100	0.25	69	69	69	5
	overall	15	12	100	—	49	81	68.4	—
RD-2	low	0	—	—	—	—	—	—	—
	med	6	35	57	1.3	69.9	72.8	71.1	10
	high	0	—	—	—	—	—	—	—
	overall	6	35	57	1.3	69.9	72.8	71.1	10
RD-3	low	10	12	12	0.5	54.9	110.7	93.7	46[c]
	med	10	40	40	0.5	79.6	89.6	82.1	6.5[c]
	high	10	124	126	0.5	72.0	74.6	73.6	1.6
	overall	30	12	126	—	54.9	110.7	83.1	—
RD-4	low	1	18[e]	18	2.0	76.1	76.1	76.1	19
	med	2	35	42	1.8[c]	67.5	71.8	69.7	12.5[c]
	high	0	—	—	—	—	—	—	—
	overall	3	18	42	—	67.5	76.1	71.8	—
RF-1	low	9	10	10	0.2	67.4	71.7	68.0	7.5[c,f]
	med	11	32	33	0.2	68.3	70.4	68.8	7.4[c,f]
	high	9	101	101	0.2	70.0	72.4	70.5	7.2[c,f]
	overall	29	10	101	—	67.4	72.4	69.06	—
RF-3	low	0	—	—	—	—	—	—	—
	med	12	35	57	1.3	69.3	73.6	72.0	10
	high	6	70	71	1.3	69.2	69.8	69.5	10
	overall	18	35	71	—	69.2	73.6	71.14	—
RF-4	low	11/24	9	14	0.41	66.1	72.8	69.4	4.5
	med	12/26	36	48	0.25	67.2	71.6	69.3	4.1
	high	12/26	68	87	0.59	67.8	71.9	70.2	4.8
	overall	35/76	9	87	—	66.1	72.8	69.7	—

Code[a]	Power[b] Range	No. of Data	Applied Voltage			Radiation Conductance			
			Min	Max	U_V	Min	Max	Avg.	U_b
			V	V	±%	μS	μS	μS	±%
RM-1	low	25	7	19	0.2	69.3	70.8	70.4	2.8
	med	16	20	58	0.2	70.3	70.7	70.5	2.8
	high	17	61	112	0.2	69.3	71.0	70.7	2.8
	overall	58	7	112	—	69.3	71.0	70.5	—
C-5	low	3	14	14	1.3	71.5	75.7	74.3	10
	med	6	35	62	1.3	66.5	70.7	69.5	10
	high	0	—	—	—	—	—	—	—
	overall	9	14	62	—	66.5	75.7	71.1	—
T-1	j	1	j	j	na	na	na	69.9	1
Q-4	j	10	j	j	i	i	i	64.5	i
R-2[k]	low	6	12	16	i	67	69	68	17
	med	0	—	—	—	—	—	—	—
	high	0	—	—	—	—	—	—	—
	overall	6	12	16	—	67	69	68	
			weighted mean[p]					70.13	

*Footnotes follow table 5.

TABLE 5. *Transfer standard No. 3-22 nominal frequency 5 MHz*.

Code[a]	Power[b] Range	No. of Data	Applied Voltage			Radiation Conductance			
			Min	Max	U_V	Min	Max	Avg.	U_b
			V	V	±%	μS	μS	μS	±%
RD-1	low	5	12	12	0.25	69	97	75	22
	med	5	40	40	0.25	77	80	78	7
	high	5	100	100	0.25	69.1	69.1	69.1	5
	overall	15	12	100	—	69	97	74.2	—
RD-2	low	0	—	—	—	—	—	—	—
	med	6	35	57	1.3	70.1	72.8	72.1	10
	high	0	—	—	—	—	—	—	—
	overall	6	35	57	1.3	70.1	72.8	72.1	
RD-3	low	10	12	12	0.5	63.2	126.3	119.7	62[c]
	med	10	40	40	0.5	75.6	93.1	80.9	6.6[c]
	high	10	124	126	0.5	85.8	89.9	87.9	1.5
	overall	30	12	126	—	63.2	126.3	96.2[o]	—
RD-4	low	1	18[e]	18	2.0	71.7	71.7	71.7	20
	med	2	35	42	1.8	66.0	71.8	68.9	13
	high	0	—	—	—	—	—	—	—
	overall	3	18	42	—	66.0	71.8	69.8	—

Code[a]	Power[b] Range	No. of Data	Applied Voltage			Radiation Conductance			
			Min	Max	U_V	Min	Max	Avg.	U_b
			V	V	±%	μS	μS	μS	±%
RF-1	low	12	10	10	0.2	71.2	71.2	71.2	7[c,f]
	med	15	32	33	0.2	71.6	72.6	71.7	7[c,f]
	high	13	101	101	0.2	73.0	73.0	73.0	7.4[c,f]
	overall	40	10	101	—	71.2	73.0	71.97	—
RF-3	low	0	—	—	—	—	—	—	—
	med	6	35	56	1.3	72.7	74.5	73.6	10
	high	3	70	70	1.3	72.4	72.5	72.5	10
	overall	9	35	70	—	72.4	74.5	73.22	—
RF-4	low	17/44[g]	8	14	0.41	68.4	78.6	72.7	4.5
	med	16/42	33	49	0.25	69.4	75.1	72.3	4.1
	high	17/44	65	107	0.59	69.9	76.5	73.4	4.8
	overall	50/130	8	107	—	68.4	78.6	72.81	—
RM-1	low	26	7	18	0.2	72.0	74.3	72.8	2.8
	med	16	20	57	0.2	72.3	73.3	72.8	2.8
	high	22	61	111	6.2	72.2	72.7	72.5	2.8
	overall	64	7	111	—	72.0	74.3	72.68	—
C-3[h]	i	i	i	i	—	i	i	73	25
C-5	low	3	14	14	1.3	71.5	72.9	72.0	10
	med	6	35	57	1.3	68.5	74.8	71.3	10
	high	0	—	—	—	—	—	—	—
	overall	9	14	57	—	68.5	74.8	71.52	—
T-1	j	1	j	j	na	na	na	72.5	1
Q-4	j	10	j	j	i	i	i	67.6	i
R-2[k]	low	2	12	17	i	68	69	69	17
	med	2	32	42	i	64	71	67	17
	high	0	—	—	—	—	—	—	—
	overall	4	12	42	—	64	71	68.0	—
			weighted mean[p]					72.22	

[a]See table 1.
[b]See "Procedures and Instructions" in Appendix.
[c]The error is not the same for all measurements; the median is given.
[d]The average is badly biased by the poor accuracy of the low-power values. If these are disregarded as outliers the average value is 11.45.
[e]All voltages in this group were reported as peak-to-peak and converted to rms by the pilot laboratory.
[f]The estimated errors were not symmetrical, that is, the positive values were not quite equal to the negative.
[g]For RF-4, the first number, e.g., 9, is the number of independent groups into which the second number, e.g., 20, which is the number of measurements, is divided. Furthermore, each of the (say) 20 measurements is the average of 4 power readings at the same voltage, two taken as the voltage was switched on, and two as it was switched off.
[h]System described as "relatively unproven."
[i]Not given.
[j]Not given but very low.
[k]According to the investigator, "These results are included for the record but are not regarded as part of the principal measurements."
[m]Same as (d) but average is 12.25.
[n]The investigator considers that the data form two independent groups, here designated—.1 and—.2. He suspects that transducer no. 3-18 suffered a physical change between runs.
[o]Same as (d) but average is 84.4.
[p]Calculated from the "overall" values and their ranges by the method given in the text.

TABLE 6. *Deviation of radiation conductance from grand average.*

Code[a]	Power[b] Range	No. of[c] Data	Deviation, $(\bar{G}_r-\bar{\bar{G}}_r)/\bar{\bar{G}}_r$ in percent											
			3-16			3-18			3-20			3-22		
			Min	Max	Avg.	Min	Max	Avg.	Min	Max	Avg.	Min	Max	Avg.
RD-1	low	5,5,5,5	−21	4.9	−3.8	−28	−10	−19	−30	−4.5	−17	−4.5	34	3.8
	med	5,5,5,5	0.5	4.0	1.4	−0.2	0.7	0.7	11	15	11	6.6	11	8.0
	high	5,5,5,5	4.9	6.6	5.8	5.2	7.0	−6.1	−1.6	−1.6	−1.6	−4.3	−4.3	−4.3
	overall	15,15,15,15	−21	6.6	0.9	−28	7.0	−4.1	−30	15	−2.5	−4.5	34	2.7
RD-2	low	3,3,0,0	2.3	3.1	3.1	6.1	7.0	7.0	—	—	—	—	—	—
	med	12,12,6,6	−2.1	4.0	0.5	0.7	6.1	3.4	−0.3	3.8	1.4	−2.9	0.8	−0.2
	high	0,0,0,0	—	—	—	—	—	—	—	—	—	—	—	—
	overall	15,15,6,6	−2.1	4.0	1.2	0.7	7.0	4.0	−3.0	3.8	1.4	−2.9	0.8	−0.2
RD-3	low	10,10,10,10	118	237	161	47	287	182	−22	58	34	−12	75	66
	med	10,10,10,10	−9.1	10.1	−4.7	13	26	19	13	28	17	4.7	29	12
	high	10,10,10,10	0.5	10.1	4.9	0.7	3.4	1.6	2.7	6.4	4.9	19	24	22
	overall	30,30,30,30	−9.1	237	54[d]	0.7	287	68[m]	−22	58	18	−12	75	33
RD-4	low	1,1,1,1	−19	−19	−19	−8.3	−8.3	.3	8.5	8.5	8.5	−0.7	−0.7	−0.7
	med	2,2,2,2	−5.6	2.3	−2.1	5.6	2.5	1	−3.7	2.4	−0.6	−8.6	−0.6	−4.6
	high	0,0,0,0	—	—	—	—	—	—	—	—	—	—	—	—
	overall	3,3,3,3	−19	2.3	−7.3	−8.3	2.5	−3.8	−3.7	8.5	2.4	−8.6	−0.6	−3.4
RF-1	low	6,7,9,12	−7.3	−2.7	−4.7	−10	−2.9	−6.5	−3.9	2.2	−3.0	−1.4	−1.4	−1.4
	med	6,7,11,15	−4.7	−2.1	−3.8	−10	−3.8	−7.4	−2.6	0.4	−1.9	−0.9	0.5	−0.7
	high	7,7,9,13	−3.0	3.1	−0.3	−5.6	−0.2	−3.8	−0.2	3.2	0.5	1.1	1.1	1.1
	overall	19,21,29,40	−7.3	3.1	−2.7	−10	−0.2	−6.0	−3.9	3.2	−1.5	−1.4	1.1	−0.3
RF-3	low	3,3,0,0	2.3	3.1	2.3	−1.1	1.6	0.7	—	—	—	—	—	—
	med	6,6,12,6	4.0	4.9	4.0	2.5	3.4	2.5	−1.2	4.9	2.7	0.7	3.2	1.9
	high	0,0,6,3	—	—	—	—	—	—	−1.3	−0.5	−0.9	0.2	0.4	0.4
	overall	9,9,18,9	2.3	4.9	3.7	−1.1	3.4	2.1	−1.3	4.9	1.4	0.2	3.2	1.4
RF-4	low	20,0,24,44	−10	−2.1	−4.7	—	—	—	−5.7	3.8	−1.0	−5.3	8.8	0.7
	med	20,0,26,42	−9.1	−1.2	−4.7	—	—	—	−4.2	2.1	−1.2	−3.9	4.0	0.1
	high	20,0,26,44	−8.2	−2.1	−4.7	—	—	—	−3.3	2.5	0.1	−3.2	5.9	1.6
	overall	60,0,76,130	−10	−1.2	−5.0	—	—	—	−5.7	3.8	−0.6	−5.3	8.8	0.8
RF-4.1[n]	low	0,26,0,0	—	—	—	−0.7	12	5.2	—	—	—	—	—	—
	med	0,26,0,0	—	—	—	−0.2	5.2	2.5	—	—	—	—	—	—
	high	0,22,0,0	—	—	—	6.1	9.7	7.0	—	—	—	—	—	—
	overall	0,74,0,0	—	—	—	−0.2	12	4.8	—	—	—	—	—	—
RF-4.2[n]	low	0,20,0,0	—	—	—	−7.4	−1.1	−3.8	—	—	—	—	—	—
	med	0,20,0,0	—	—	—	−7.4	−2.0	−4.7	—	—	—	—	—	—
	high	0,20,0,0	—	—	—	−6.5	−2.0	−3.8	—	—	—	—	—	—
	overall	0,60,0,0	—	—	—	−7.4	−1.1	−4.2	—	—	—	—	—	—
RM-1	low	34,32,25,26	−2.1	0.5	−0.3	−1.1	1.6	0.7	−1.2	1.0	0.4	−0.3	2.9	0.8
	med	15,13,16,16	−1.2	−1.2	−1.2	−1.1	0.7	−0.2	0.2	0.8	0.5	0.1	1.5	0.8
	high	17,19,17,22	−1.2	−1.2	−1.2	−1.1	2.5	0.7	0.1	1.2	0.8	0.0	0.7	0.4
	overall	66,64,58,64	−2.1	0.5	−0.9	−1.1	2.5	0.4	−1.2	1.2	0.5	−0.3	2.9	0.6
C-3	h	i,i,i,i,	i	i	−3.0	—	—	—	—	—	—	i	i	1.1
C-5	low	3,3,3,3	−1.2	7.5	3.1	1.6	7.0	3.4	2.0	7.9	5.9	−1.0	0.9	−0.3
	med	3,3,6,6	3.1	8.4	5.8	−2.0	9.7	3.4	−5.2	0.8	−0.9	−5.2	3.6	−1.3
	high	0,0,0,0	—	—	—	—	—	—	—	—	—	—	—	—
	overall	6,6,9,9	−1.2	8.4	4.4	−2.0	9.7	3.4	−5.2	7.9	1.4	−5.2	3.6	−1.0

Code[a]	Power[b] Range	No. of[c] Data	Deviation, $(\bar{G}_r\text{-}\bar{\bar{G}}_r)/\bar{G}_r$ in percent											
			3-16			3-18			3-20			3-22		
			Min	Max	Avg.	Min	Max	Avg.	Min	Max	Avg.	Min	Max	Avg.
0-1	low	0,0,0,0	—	—	—	—	—	—	—	—	—	—	—	—
	med	9,9,0,0	-7.3	5.8	-1.2	-2.9	7.0	2.5	—	—	—	—	—	—
	high	5,6,0,0	-4.7	2.3	-1.2	-2.9	3.4	1.6	—	—	—	—	—	—
	overall	14,15,0,0	-7.3	5.8	-1.3	-2.9	7.0	1.9	—	—	—	—	—	—
T-1		0,0,1,1	—	—	—	—	—	—	na	na	-0.3	na	na	0.4
Q-4		10,10,10,10	i	i	-7.7	i	i	-7.9	i	i	-8.0	i	i	-6.4
R-2[k]	low	6,0,6,2	-4.7	0.5	-3.0	—	—	—	-4.5	-1.6	-3.0	-5.8	-4.5	-4.5
	med	0,0,0,2	—	—	—	—	—	—	—	—	—	-11	-1.7	-7.2
	high	0,0,0,0	—	—	—	—	—	—	—	—	—	—	—	—
	overall	6,0,6,4	-4.7	0.5	-3.0	—	—	—	-4.5	-1.6	-3.0	-11	-1.7	-5.8
R-2.1	low	0,2,0,0	—	—	—	-4.7	-2.0	-3.8	—	—	—	—	—	—
	med	0,0,0,0	—	—	—	—	—	—	—	—	—	—	—	—
	high	0,0,0,0	—	—	—	—	—	—	—	—	—	—	—	—
	overall	0,2,0,0	—	—	—	-4.7	-2.0	-3.8	—	—	—	—	—	—
R-2.2	low	0,1,0,0	—	—	—	8.8	8.8	8.8	—	—	—	—	—	—
	med	0,0,0,0	—	—	—	—	—	—	—	—	—	—	—	—
	high	0,0,0,0	—	—	—	—	—	—	—	—	—	—	—	—
	overall	0,1,0,0	—	—	—	8.8	8.8	8.8	—	—	—	—	—	—

[a,b,k,h, and n]See footnotes to tables 2,3,4, and 5.
[c]For 3-16, 18, 20, and 22 respectively.
[d]This average is badly biased by the poor accuracy of the low-power values. If these are disregarded as outliers, the value becomes -0.1%.
[m]Same as [d] but value becomes 10%.
[o]Same as [d] but value is 17%.

TABLE 7. *Cumulative distribution of the deviations of tables 2, 3, 4, and 5.*

	No. of cases for which $(\bar{G}_r\text{-}\bar{\bar{G}}_r)/\bar{G}_r<\Delta$			
Frequency, MHz	2		5	
$\dfrac{\Delta}{\%}$	No.	Fraction of total %	No.	Fraction of total %
1	3	11	10	40
2	6	22	17	68
3	9	33	20	80
4	14	52	21	84
5	19	70	21	84
6	20	74	22	88
7	21	78	23	92
8	24	89	23	92
9	25	93	23	92
∞	27	100	25	100

(although a 3- rather than a 2-MHz unit) exhibited a large shift in the measured G_r. Upon autopsy it was found to have suffered a small crack in the epoxy seal and therefore a small leak. Upon being dried out and recemented the transducer yielded its original G_r.

One could speculate that a small leak occurred while transducer 3-18 was at the participant's laboratory and that on the way back to the pilot laboratory the transducer dried out. Sixteen months later, when the last measurements were made, the transducer was still behaving properly, at least under the pilot laboratory conditions. While we were at it, we took additional measurements on the other transducers as well. All of the measurements made by the modulation radiation-pressure method at the pilot laboratory are summarized in table 8.

From the material in table 8, we could conclude that whatever drifts occur in either the transducers or the ap-

paratus itself are of no great consequence. However, close examination, using standard statistical tests, shows that the disparities are not entirely random. Indeed, the regressions of G_r on time show trends which are significant although not overwhelmingly so. To elucidate this question will require a carefully planned experimental design carried out over several years, and this is under serious consideration.

TABLE 8. *Summary of radiation conductance, G_r.*

	2 MHz		5 MHz	
Transducer	3-16	3-18	3-20	3-22
n (over about 1233 days)	87	85	79	85
$\overline{\overline{G}}_r$ (Grand average) μS	11.352	11.150	70.42	72.36
Standard deviation				
μS	0.075	0.106	0.21	0.40
%	0.51	0.95	0.31	0.55

5. References

[1] Zapf, Thomas L. Calibration of quartz transducers as ultrasonic power standards by an electrical method. IEEE Ultrasonics Symposium Proceedings: Cat. # 74 CHO ISU; 1974; 45-49.
[2] Greenspan, M., Breckenridge, F.R., Tschiegg, C.E. Ultrasonic transducer power output by modulated radiation pressure. J. Acoust. Soc. Am. 63(4): 1031-1038; 1978.
[3] Zapf, T.L., Harvey, M.E., Larsen, N.T., Stoltenberg, R.T. Ultrasonic calorimeter for beam power measurements. Natl. Bur. Stand. (U.S.) Tech. Note 686; 1976 September. 36 p.
[4] Snedecor, George W. Statistical methods, 6 ed. Ames: Iowa State University Press; 1967. 593 p.

6. Appendix

International Intercomparison of cw Ultrasonic Beam Power Measurements — Procedures and Instructions

National Bureau of Standards
Washington, DC 20234

This document provides instructions and a typical procedure for the intercomparison of ultrasonic beam power measurements. The intercomparison is being conducted by circulating to participating laboratories four transfer standards, namely, half-wave resonant, air-backed, quartz transducers.

6.1 Equipment Supplied by NBS

1. Transfer standards. The resonance frequencies of the transducers have been measured at NBS.
2. Matching circuit. A matching circuit may be needed to provide adequate voltage to the quartz transducers, which have a high electrical input impedance. It also helps to minimize distortion in the voltage applied to the transducers.
3. Connectors. Adapters are supplied for use with the transducers.

6.2 Care of the Standard Transducers

1. Avoid any severe mechanical shock.
2. Voltage limitations on the transducers are 3 V unloaded, and 350 V water loaded. Transducer voltage should be monitored at all times when connected to a power amplifier. Experimental procedures should be used that will ensure that the test voltage is not applied when the transducer is out of water and that the voltage is removed before removing the transducer from the water.
3. The transducer connectors are not waterproof, and should not be submerged.
4. The front faces of the transducers are gold plated. They should be carefully wiped with lens tissue to remove water. Avoid excessive force.

6.3 Measurements To Be Made

The quantity to be measured is the total cw beam power radiated by a transducer (the supplied transfer standard) into a reflectionless water load at a specified temperature, frequency, and sinusoidal input voltage to the transducer. At the power levels to be used in the intercomparison, the beam power is proportional to the square of the applied voltage. Each participant is responsible for obtaining a suitable rf voltmeter and having it calibrated at the voltages and frequencies required. The following table indicates the specified frequency, f_s, and the specified voltage, V_s, at which each measurement is to be made. The actual frequency, f_m, of the measurement should be within $\pm 0.02\%$ of f_s. The measured voltage, V_m, should be within $\pm 50\%$ of V_s (subject to the 350 V maximum limitation). The voltages are arbitrary, but have been chosen to cover the range of interest.

6.4 Reporting

Please use the reporting form included herewith. Report the test data in the sequence in which the data

were taken.

The pilot laboratory will accumulate and summarize the results from all participating laboratories. As discussed in the following paragraphs, numerical results from each participant should be reported in a manner to allow comparison on a common basis.

An error can result from attenuation in the water coupling medium between the transducer and the receiver target. The radiated beam power, P_r, equals the received power measured by the participant's equipment, P_m, plus the power loss in the coupling medium. This loss should be determined by measurement or calculation, and applied as a correction as indicated below. To correct for the attenuation, the following formula may be used:

$$P_r = P_m \cdot \exp 44 \times 10^{-17} f_m^2 d,$$

where d is the water path distance in centimeters between the transducer and the point at which the power measurement is made, and f_m is the measurement frequency in Hz.

The temperature of the water coupling medium should be as close as possible to 23 °C, and in the range of 20 °C to 26 °C. A correction to a common-basis temperature and voltage should be applied as follows:

$$P_b = P_r (V_s/V_m)^2 [1 + 0.0016 (T_m - 23)],$$

where P_b is the "common basis power" that would be measured at 23 °C with the common basis voltage, V_s, applied to the transducer, V_m is the measured applied voltage, T_m is the measurement temperature in °C. The coefficient 0.0016 is related to the temperature dependence of the ϱc of water.

So that the fractional uncertainty, U_b, associated with the common-basis power is properly determined at each test point, the participant should estimate the fractional uncertainty, U_r, in the radiated power, taking into account the uncertainty in measuring or calculating the loss in the coupling medium. For example, if P_r is 0.137 watts and the uncertainty in P_r is ±0.004 watts, then U_r = ±0.004/0.137 = ±0.03, or ±3%. The common-basis power uncertainty, U_b, is then calculated as

$$U_b = U_r + 2U_v$$

where U_v is the fractional uncertainty in the voltmeter calibration and the factor 2 is a result of the square-law relationship between voltage and power. Uncertainties associated with the application of the temperature correction will be negligible if temperatures are kept within the specified range. The estimate of U_r should be based on the participant's experience with his equipment; it should not be influenced by the variations observed in the present intercomparison.

Provide a brief description of each set of equipment and method of measurement used in the intercomparison. If more than one method of measurement is used, please report each on a separate data sheet.

If the quantities V_m and P_m are inappropriate to the method of measurement used, then please supply at least the following information for each measurement: temperature of the measurement, T_m; frequency of the measurement, f_m; the radiation conductance, G_r, measured for the transducer; and the estimated uncertainty, U_b, of the measured G_r.

6.5 Precautions

The transducer must be oriented so that the entire ultrasonic beam will be received by the participant's measuring equipment. Reflections that would cause ultrasonic energy to return to the transducer must be reduced to a negligible level to prevent interference at the face of the transducer that may change the characteristics of the transfer standard.

Care should be exercised to avoid the presence or formation of bubbles on the transducer face during test. The use of degassed water may eliminate this problem.

6.6 Typical Procedure

The following information is included but may be disregarded if not applicable:

Typical equipment provided by participants:
1. Voltmeter. A radio-frequency voltmeter is needed to measure the voltage applied to the transducers. The voltmeter must be calibrated at the frequencies and voltages listed under *Measurements to be made*. The voltmeter should be calibrated with a short cable. This will minimize loading on the matching network. This cable then becomes part of the calibrated voltmeter. A calibration uncertainty of ±0.25% or better is desirable.
2. Power amplifier. A power amplifier capable of supplying 5 watts into a 50-ohm load should be adequate.
3. Signal generator. A stable generator must drive the power amplifier with a cw sinusoidal waveform of low distortion (preferably less than 0.5%).
4. Frequency counter. This is needed to set the frequency of the signal applied to the transducer.

Typical procedure

1. Interconnect equipment as indicated in figure A-1, but *do not turn on* the signal generator and power amplifier before first setting the output level controls to minimum. NOTE: CONNECTORS ON THE TRANSDUCERS ARE NOT WATER-PROOF AND *MUST BE PROTECTED IF IM-MERSED IN WATER*.
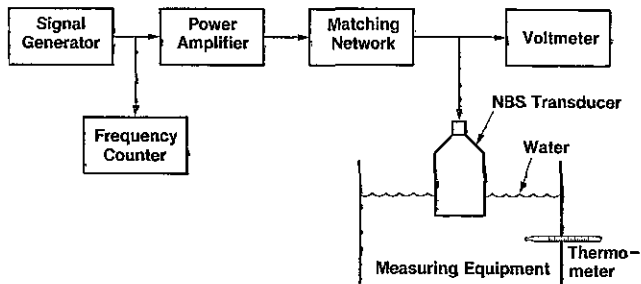
FIGURE A-1. Example of possible test assembly.

2. Prepare the measuring equipment for measurements of power at a temperature of 23 °C $+3°$.

3. Place the NBS transducer in the water coupling port of the measuring equipment. Brush away any bubbles adhering to the face of the transducer. CAU-TION — DO NOT APPLY VOLTAGE TO TRANSDUCER UNLESS THE GOLD TRANSDUCER FACE IS IN THE WATER (i.e., THE TRANSDUCER IS LOADED). AP-PLICATION OF HIGH VOLTAGE TO AN UNLOADED QUARTZ TRANSDUCER (i.e., IN AIR) MAY DAMAGE IT.

4. Set the signal generator controls to obtain a cw sinusoidal waveform. Set the frequency controls of the signal generator approximately to the specified resonance frequency (loaded) of the NBS transducer. Adjust the measurement frequency, f_m, to within $\pm 0.02\%$ of the specified resonance frequency f_s, of the transducer using the frequency counter as an indicator. Frequency should be monitored continuously during the test and adjusted, whenever necessary.

5. Set the voltmeter range switch to a suitable low voltage range. Increase the signal generator output to obtain a reading of perhaps 3 to 10 volts. Adjust the controls in the matching-circuit to obtain maximum voltage, *being careful not to exceed 3 volts unloaded to 350 volts water loaded* (if necessary reduce the signal from the generator).

6. The signal can now be increased to a desired test level. Table A-1 gives the *test points* (in terms of frequency and voltage) at which measurements are to be made by all participants. The number of measurements to be made at each point is not specified, although a number from 3 to 10 would seem practical.

TABLE A-1

Transducer No.	Frequency f_s, MHz	Specified voltages, V_s
3-16	1.995	30-100-300
3-18	1.995	30-100-300
3-20	5.0457	12-40-125
3-22	5.0148	12-40-125

The Efficiency of the Biweight as a Robust Estimator of Location

Karen Kafadar*

National Bureau of Standards, Washington, DC 20234

The biweight is one member of the family of M-estimators used to estimate location. The variance of this estimator is calculated via Monte Carlo simulation for samples of sizes 5, 10, and 20. The scale factors and tuning constants used in the definition of the biweight are varied to determine their effects on the variance. A measure of efficiency for three distributional situations (Gaussian and two stretched-tailed distributions) is determined. Using a biweight scale and a tuning constant of $c = 6$, the biweight attains an efficiency of 98.2% for samples of size 20 from the Gaussian distribution. The minimum efficiency at $n = 20$ using the biweight scale and $c = 4$ is 84.7%, revealing that the biweight performs well even when the underlying distibution of the samples has abnormally stretched tails.

Key words: bisquare weight function; biweight scale estimate; median absolute deviation; M-estimator; tuning constant.

1. Introduction

Robust estimation of location has become an important tool of the data analyst, due to the recognition among statisticians that parametric models are rarely absolutely precise. Much discussion has taken place to determine the "best" estimators ("best" in a certain sense, such as low variance across several distributional situations). Estimators which were designed to be robust against departures from the Gaussian distribution in a symmetric, long-tailed fashion were investigated in-depth by Andrews et al. in 1970-1971 [1].[1] Subsequent to this, Gross and Tukey compared several other estimators in the same fashion, one of which they called the biweight [2]. It was designed to be highly efficient in the Gaussian situation as well as in other symmetric, long-tailed situations. The first reference of its practical use appears two years later [3]. Gross showed that the biweight proves useful in the "t"-like confidence interval for the one-sample problem [4] and for estimating regression coefficients [5]; Kafadar showed that it is efficient for the two-sample problem also [6].

Many scientists collect data and perform elementary statistical analyses but seldom use summary statistics other than the sample mean and sample standard deviation. This paper is therefore addressed to two audiences. It provides a brief introduction to the field of robust estimation of location to explain the biweight in particular (section 2). Those who are familiar with the basic concepts may wish to proceed directly to section 3 which raises the specific questions about the biweight's computation and efficiency that are answered in this paper. Section 4 describes the results of a Monte Carlo evaluation of the biweight. An example to illustrate the biweight calculation is presented in section 5, followed by a summary in section 6.

2. Robust Estimation of Location; M-Estimates.

Given a random sample of n observations, $X_1,...,X_n$, typically one assumes that they are distributed independently according to some probability distribution with a finite mean and variance. For convenience, the Gaussian distribution is the most popular candidate; representing its mean and variance by μ and σ^2, it is well known that the ordinary sample mean and sample variance are "good" estimates, in that, on the average, they estimate μ and σ^2 unbiasedly and with minimum

---

*Center for Applied Mathematics, National Engineering Laboratory.
[1]Figures in brackets indicate literature references at the end of this paper.

variance. Often, however, this Gaussian assumption is not exactly true, owing to a variety of reasons (e.g., measurement errors, outliers). Ideally, such departures from the assumed model should cause only small errors in the final conclusions. Such is not the case with the sample mean and sample variance; even one misspecified observation can throw these estimates far from the true μ and σ^2 (e.g., see Tukey's example in [7]).

It is important, then, to find alternative estimators of location and scale. Huber [8, p. 5] lists three desirable features of a statistical procedure:

1. reasonably efficient at the assumed model;
2. large changes in a small part of the data or small changes in a large part of the data should cause only small changes in the result (resistant);
3. gross deviations from the model should not severely decrease its efficiency (robust).

A class of estimators, called M-estimators, was proposed by Huber [9] to satisfy these three criteria. This class includes the sample mean in the following way. Let T be the estimate which minimizes

$$\sum_{i=1}^{n} \varrho(X_i - T) \qquad (1)$$

where ϱ is an arbitrary function. If $\Psi(x-\mu) = (\partial / \partial \mu)\varrho(x-\mu)$, then T may also be defined implicitly by the equation

$$\sum_{i=1}^{n} \Psi(X_i - T) = 0. \qquad (1')$$

(There may be more solutions to (1'), however, corresponding to local minima of (1).)

If $\varrho(u) = u^2$, then (1) defines the sample mean $\overline{X}$ (and $\overline{X}$ is therefore called least squares estimate). It can be shown that M-estimates are maximum likelihood estimates (MLE) when $X_1,...,X_n$ have a density proportional to $\exp\{-\int \Psi(u)du\}$ (e.g., $\overline{X}$ is MLE for the Gaussian distribution), but their real virtue is determined by their robustness in the face of possible departures from an assumed Gaussian model. Many suggestions for Ψ have been offered, one of which is the biweight Ψ-function:

$$\Psi(u) \quad = \quad u(1-u^2)^2 \qquad |u| \leqslant 1$$
$$\qquad \qquad = \quad 0 \qquad \qquad \text{otherwise.} \qquad (2)$$

Using (2), T as defined by (1') is called the biweight. Actually, the solution in this form is not scale invariant.

We therefore define the biweight as the solution to the scale-invariant equation

$$\sum_{i=1}^{n} \Psi[(X_i - T)/(cs)] = 0, \qquad (3)$$

where s is a measure of scale of the sample and c is any positive constant, commonly called the "tuning constant." A graph of the biweight Ψ function (2) is shown in figure 1.
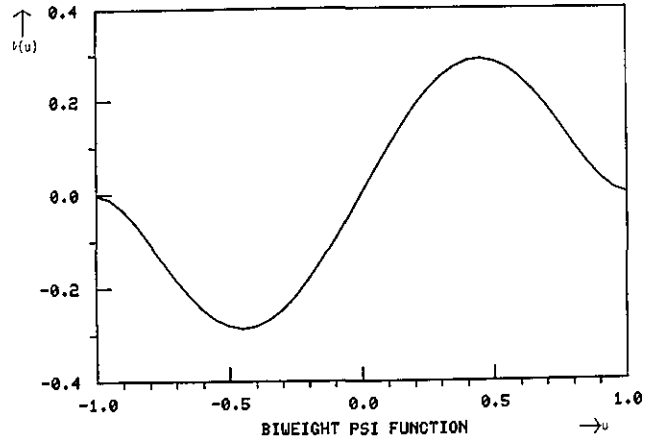
FIGURE 1

The lack of monotonicity in the biweight Ψ-function leads to its inclusion in the class of the so-called "redescending M-estimates," a term first introduced by Hampel [1, p. 14]. Typically, the defining Ψ-functions have finite support (i.e., are 0 outside a finite interval); hence, redescending M-estimates have the property that the calculation assigns zero weight to any observation which is more than c multiples of the width from the estimated location. To see this, we define the weight function corresponding to any M-estimate, $w(\cdot)$, by the following equation:

$$w(u) = \Psi(u)/u.$$

Hence, (3) becomes

$$0 = \Sigma\,[(X_i - T)/(cs)] \cdot w[(X_i - T)/(cs)]$$

which implies

$$T = \Sigma\,X_i w(u_i)/\Sigma\,w(u_i) \qquad (4)$$

where

$$u_i = (X_i - T)/(cs).$$

Equation (4) reveals that the calculation of T may be viewed as an iteratively reweighted average of the observations. A graph of the weight function used for the biweight,

$$w(u) \quad = \quad (1-u^2)^2 \qquad |u| \leqslant 1$$

$$\quad = \quad 0 \qquad\qquad \text{otherwise,}$$

also known as the bisquare weight function, is shown in figure 2, where it is clear that zero weight is assigned to any value outside $(T - cs, T + cs)$. Henceforth, Ψ and w will always refer to the biweight M-estimator.
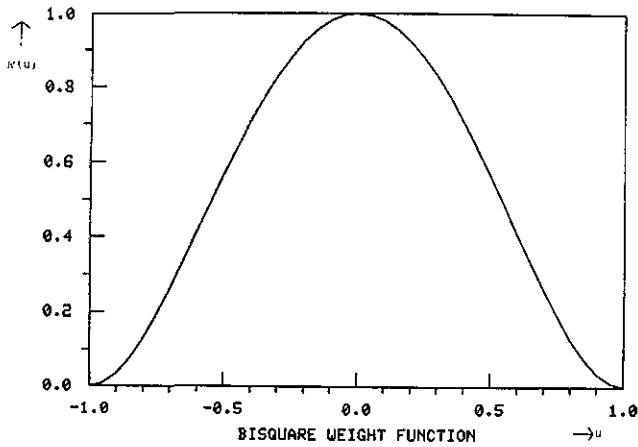
FIGURE 2

Because of the non-monotonicity of the biweight Ψ-function, multiple solutions to (3) are possible. It has been argued that an iteration based on (4) will not converge to all of the solutions to (3) and therefore will not get trapped by local minima of (1) [10]. In addition, the iteration suggested by eq (4) is more stable than a root finding search suggested by (3). These two facts encourage the use of (4), called the w-iteration, in calculating T.

3. Use of the Biweight in Practice

There has been considerable discussion on the practical usefulness of the biweight, and of redescending M-estimates in general. Huber points out that they are more sensitive to scaling (i.e., prior estimation of s in (4)), and warns of possible problems in convergence [8, pp. 102-103]. In addition, unlike the monotone Ψ-functions, an estimate defined by a redescending Ψ-function is not a maximum likelihood estimate for any density function, for it is constant outside a finite interval and hence does not integrate to 1. The central (non-constant) part of what would be the corresponding density $(\exp(-\int\Psi(u)du))$, scaled to have the same density at 0 as the unit Gaussian, reveals "shoulders" (Fig. 3), which may or may not correspond to realistic applications.
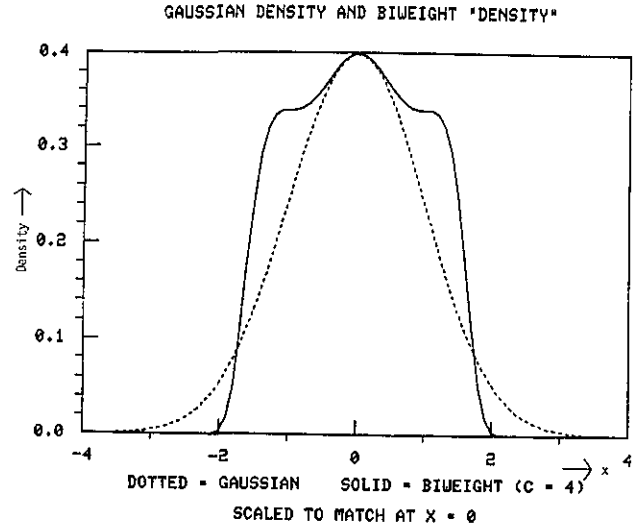
FIGURE 3

Nonetheless, the popularization of the biweight demands a careful assessment of its performance. This paper, therefore, documents its efficiency in three distributional situations using small- to moderate-sized samples.

The study reported below involved a Monte Carlo simulation of three situations, and three sample sizes, in order to determine the variance of the biweight using four different scalings and seven different values of the tuning constant. This section provides details on the calculation of the biweight, a description of the underlying situations in the Monte Carlo study, and the efficiency criterion on which it was evaluated.

3.1 Calculation and Scalings

Taking (3) as the definition of T for this study, we calculate the biweight iteratively: after the kth iteration,

$$T^{(k+1)} = \frac{\Sigma X_i \, w[(X_i - T^{(k)})/(cs)]}{\Sigma w[(X_i - T^{(k)})/(cs)]}, \quad k = 0,1,2\dots . \quad (5)$$

One may begin the iteration with any robust estimate of location. For this study, $T^{(0)}$ is the median for reasons of convenience and computational ease. In this form, the scale estimate remains fixed throughout the iteration. One may also consider updates on the scale:

$$T^{(k+1)} = \frac{\Sigma\, X_i\, w[(X_i - T^{(k)})/(cs^{(k)})]}{\Sigma\, w[(X_i - T^{(k)})/(cs^{(k)})]}\ ,\quad k = 0,1,2\ldots . \tag{6}$$

Two forms of scale functions were considered in connection with iterations (5) and (6). The median absolute deviation about the current estimate

$$s_{MAD}{}^{(k+1)} = \operatorname*{med}_{1\leqslant i\leqslant n} |\,X_i - T^{(k)}\,|,\quad T^{(0)} = \operatorname*{med}_{1\leqslant i\leqslant n} X_i \tag{7}$$

or "MAD," has been used frequently in many robustness studies, including Andrews et al. [1]. In the Gaussian situation, the average value of the MAD is roughly two thirds of the standard deviation, so we really use 1.5 x MAD. The second scale is based on a finite sample version of the theoretical asymptotic variance of T [8, p. 45]:

$$s_{bi}{}^{(k+1)} = \left(\frac{n(cs_{bi}{}^{(k)})^2\, \Sigma\Psi^2(u_i)}{[\Sigma\Psi'(u_i)]\max\,[1,\,-1 + \Sigma\Psi'(u_i)]}\right)^{1/2}$$

$$u_i = (X_i - T^{(k)})/(cs_{bi}{}^{(k)})\ . \tag{8}$$

The subscript refers to the fact that s_{bi} uses the bi-square weight function in its computation. The initial $s_{bi}{}^{(0)}$, again for reasons of convenience, is taken here as 1.5 x MAD. Equation (8) is designed to yield the ordinary sample variance when the Ψ-function is the identity (least squares); hence the use of the "−1" in the denominator. Other values besides −1 have been investigated [11] but have proved less satisfactory. Equation (5) may also proceed without any scale updates (i.e., (7) and (8) calculated once and used throughout the iteration). Figure 4 illustrates four possibilities for scale evaluated in this study.

3.2 Distributional Situations

The variance of the biweight was calculated on three distributional situations:

- Gaussian (n observations from N(0,1));
- One Wild (n-1 observations from N(0,1); 1 unidentified observation from N(0,100));
- Slash (n observations from N(0,1)/independent uniform on [0,1]).

The general term "situation" is applied particularly for the One-Wild, as the observations are not independent (n-1 "reasonable-looking" observations suggest that the next is almost sure to be "wild"). The Slash distribution is a very stretched-tailed distribution like the Cauchy,
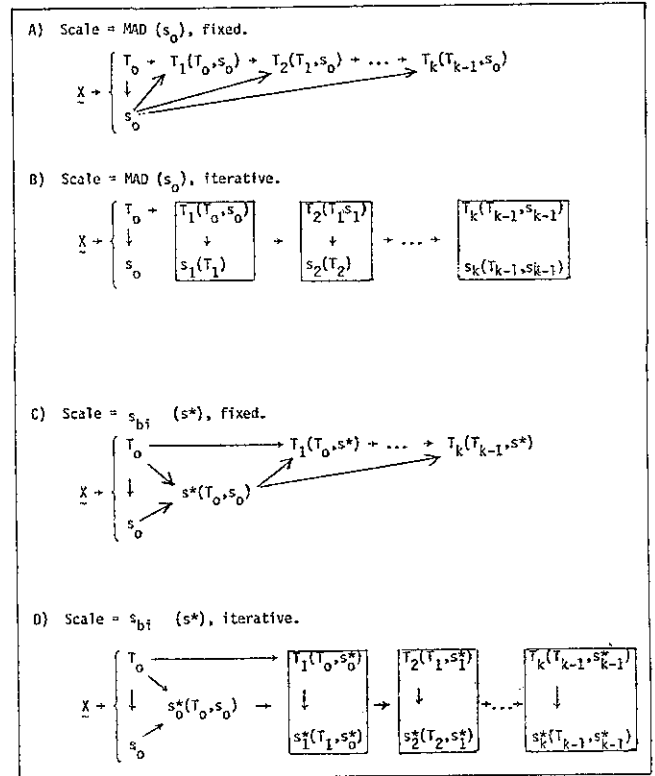
FIGURE 4. Four possible methods of iteration in the calculation of the biweight and associated scale from a sample $\underset{\sim}{X} = (X_1, \ldots, X_n)$ of n observations.

For purposes of notational clarity, the following notation is used:

T = biweight location estimate
s = MAD scale estimate (equation 7)
s^* = biweight scale estimate (equation 8)

and the subscript on each refers to the iteration at which the estimate is calculated.

but is less peaked in the center, making it a more realistic situation.

These three situations were chosen for two reasons. First, characteristics of sampling distributions of the various statistics may be estimated efficiently through a Monte Carlo swindle described by Simon [12] when the underlying distribution is of the form Gaussian/(symmetric positive distribution). Second, the three situations represent extreme types of situations for real-world applications ("utopian," outliers, and stretched tails); if an estimator performs well on these three, it is likely to perform well on almost any symmetric distribution arising in practice [13]. Additional characteristics about these distributions may be found in [14].

108

3.3 Efficiency Comparisons

In assessing the performance of a location estimator, one typically hopes for (i) unbiasedness, and (ii) minimal variance. It is simple to see that any M-estimate defined with an antisymmetric Ψ function will be unbiased in symmetric situations. Furthermore, Huber has shown that under some regularity conditions, an M-estimator has an asymptotically Gaussian distribution with a finite variance, even for underlying distributions having infinite mean and variance [8, pp. 49-50]. Thus, it is reasonable to compare the variance of the biweight with the variance of the unbiased location estimator having minimal variance, if it exists, for a given situation.

It is known that the minimal variance that is attainable for an unbiased location estimator in the Gaussian situation is simply $1/n$, or

$$\text{Var}\,(\sqrt{n}\ \overline{X}) = V_G = 1.$$

Minimal variances for the One-Wild and Slash, however, are not so simple. Theoretically, one might determine the variance of the maximum likelihood estimate for the One-Wild density but the derivation is not straightforward. A simple remedy is to pretend that one knows an observation is wild, which one it is, and eliminate it from the sample. Then the "near-optimal" variance would be

$$V_w = n/(n\text{-}1).$$

A "near-optimal" variance for the Slash density

$$
\begin{aligned}
(1/\sigma)\mathrm{f}(z) \;=\; & [1 - \exp(-z^2/2)]/(\sqrt{2\pi}\ \sigma z^2) & z \neq 0 \\
& (2\sigma\sqrt{2\pi})^{-1} & z = 0
\end{aligned}
$$

where

$$z = (X - \mu)/\sigma,$$

may be obtained through a maximum likelihood procedure. Details of this derivation may be examined in [15]. The variance of the Slash MLE, V_s, was determined within the Monte Carlo. For all three situations, the efficiency of the biweight is then calculated as

$$\text{efficiency} \;=\; \frac{\text{``minimum'' attainable variance}}{\text{variance (biweight)}}.$$

Efficiency as close to 1 (or 100%) as possible is desirable. So, sometimes it is more useful to calculate the complement, i.e., to examine how far

$$\text{deficiency} = 1 - \text{efficiency}$$

is from zero (see [1, p. 121]).

4. Results

All computations were performed on a Univac 1108. One thousand samples of sizes 5, 10, and 20 were generated. Uniform deviates were obtained using a congruential generator [16]; the Box-Muller transform was applied to these to obtain Gaussian deviates [17]. The iteration in (4) was terminated when the relative change was less than 0.0005, or if the number of iterations exceeded 15 (in which case, $T^{(15)}$ became the estimate of location).

Tables 1, 2, and 3 provide the variances, their sampling errors (SE) and deficiencies of the biweight for the Gaussian, One-Wild, and Slash situations. The most immediate observation is the low deficiency of the biweight in the Gaussian situation: using $c = 4$, as recommended in Mosteller and Tukey [18], the biweight is never more than 10% less efficient than the optimal sample mean for any of the scalings here (except $n=5$, where it loses 15% for fixed s_{bi}). As c increases, the deficiency is even lower. At $c = 6$, even for $n = 5$, the deficiency is less than 6%. As noted by Mosteller and Tukey, relative differences in deficiency of less than 10% are essentially indistinguishable in practice [18, p. 206].

Comparing the scalings, s_{bi} typically provides lower variances than does 1.5 x MAD. The only exception to this is in some of the values computed for the Gaussian, where the differences are so small as to be unimportant (at $c = 4$, largest difference = 4.9%; at $c = 6$, 2.7%). The differences in deficiency can be quite sizeable for the One-Wild and Slash situations (e.g., at $c = 4$, a difference of almost 20% for Slash, $n = 20$).

In addition, one notes that the additional computation in updating the scale estimate with each iteration is not terribly worthwhile, as deficiencies are only trivially higher in most cases. In fact, such updating can cause considerable deficiency. As a check on the convergence of the iteration, table 4 shows the number of samples, out of 1000, that did not satisfy the convergence criterion. Most of the non-convergences occurred with the iterative scales, particularly the iterative MAD.

TABLE 1. *Biweight variances and deficiencies: n=5.*

Tuning Constant	1.5xMAD — Fixed			1.5xMAD — Iterative			s_{bi} — Fixed			s_{bi} — Iterative		
	Variance	SE	Deficiency (%)	Variance	SE	Deficiency (%)	Variance	SE	Deficiency (%)	Variance	SE	Deficiency (%)
Gaussian (optimal = 1.0)												
3	1.2114	0.0172	17.5	1.1959	0.0171	16.4	1.2652	0.0203	21.0	1.2475	0.0201	21.1
4	1299	0134	11.5	1065	0130	9.6	1694	0163	14.5	1294	0149	12.6
5	0879	0109	8.1	0702	0106	6.6	1068	0132	9.6	0816	0126	8.6
6	0611	0088	5.8	0398	0082	3.8	0693	0106	6.5	0550	0104	6.1
7	0438	0072	4.2	0200	0053	2.0	0487	0090	4.6	0371	0086	4.4
8	0326	0061	3.2	0155	0045	1.5	0387	0084	3.7	0311	0082	3.8
9	0264	0057	2.6	0124	0043	1.2	0262	0070	2.6	0204	0068	2.6
One-Wild (optimal = 1.2)												
3	1.7377	0.0314	30.9	1.7064	0.0302	29.7	1.6946	0.0282	29.2	1.6979	0.0281	30.5
4	2.0164	0461	40.4	2.1890	0658	45.2	1.8322	0366	34.5	1.9621	0447	40.2
5	2.4523	0709	51.1	3.0922	1281	61.2	2.1110	0540	43.2	2.5201	0835	53.9
6	2.9642	0977	59.5	4.2740	1933	71.9	2.6146	0850	54.1	3.3286	1302	65.3
7	3.5080	1235	65.8	5.6037	2657	78.6	3.2118	1199	62.6	4.2358	1748	72.8
8	4.0822	1481	70.6	6.9447	3101	82.7	3.9072	1537	69.3	5.0837	2163	77.4
9	4.6817	1725	74.4	8.3881	3705	85.7	4.5843	1877	73.8	5.9725	2561	80.7
Slash (optimal = 10.375)												
3	22.291	5.787	53.4	21.964	6.008	52.8	22.497	6.346	53.9	22.312	5.976	63.3
4	23.470	6.034	55.8	33.974	11.664	69.5	22.618	6.006	54.1	30.965	10.533	75.0
5	25.218	6.331	58.8	37.209	12.131	72.1	26.191	7.061	60.4	33.872	11.295	77.0
6	28.207	6.981	63.2	42.045	12.466	75.3	31.643	9.610	67.2	37.952	11.764	79.1
7	31.873	3.205	67.4	45.744	12.647	77.3	34.461	10.723	69.9	39.713	12.034	80.0
8	34.778	9.289	70.2	47.387	12.743	78.1	37.223	11.570	72.1	42.677	12.312	81.1
9	36.791	10.073	71.8	52.963	13.121	80.4	39.923	12.188	74.0	45.549	12.470	82.1

Figures 5, 6, and 7 provide graphs of deficiency as a function of the tuning constant, for sample sizes $n = 5$, 10, and 20. The uncertainty limits on these graphs, plotted with dotted lines, are given by

$$1 - [\text{``minimum'' variance}]/[\text{var(biweight)} \pm \text{SE}],$$

where SE refers to the Monte Carlo sampling error in the calculation of the biweight variances. These reveal that, across these three situations, $c = 4$ to $c = 6$ is a practical value of the tuning constant, for larger values tend to yield extremely high deficiencies for the Slash.

The biweight deficiencies computed here scaled by 1.5 x MAD (fixed) differ from those computed by Holland and Welsch [19] in part because of the difference in starting value (they took $T^{(0)} = $ least absolute deviations estimate), and in convergence criterion (they took $T^{(5)}$ as their solution). Asymptotically, $c = 4.685$ yields 95% asymptotic efficiency at the Gaussian [i.e., $\sqrt{n}T$ con-

verges in distribution to $N(0, 1.0526)$]; within two sampling errors, the results in tables 1, 2, and 3 are consistent with this value.

As noted earlier, $T^{(15)}$ became the estimate of location in cases of non-convergence in the study. This only increases the variance of the biweight that we are likely to see in practice, because this situation occurred typically when the iteration alternated between two equally distant values from μ. In practice, one should examine the sample to determine the cause of non-convergence, and possibly settle on the median and 1.5 x MAD as expedient location and scale estimates.

5. An Example

To illustrate the calculation of the biweight, we use some chemical measurements collected at the National Bureau of Standards. These data were taken from

TABLE 2. *Biweight variances and deficiencies: $n=10$.*

Tuning Constant	1.5xMAD — Fixed			1.5xMAD — Iterative			s_{bi} — Fixed			s_{bi} — Iterative		
	Variance	SE	Deficiency (%)	Variance	SE	Deficiency (%)	Variance	SE	Deficiency (%)	Variance	SE	Deficiency (%)
Gaussian (optimal = 1.0)												
3	1.1250	0.0109	11.1	1.1083	0.0115	9.8	1.1937	0.0146	16.2	1.1930	0.0156	16.2
4	.0578	0075	5.5	0469	0069	4.5	0961	0099	8.8	0800	0083	7.4
5	0319	0056	3.1	0236	0051	2.3	0479	0068	4.6	0335	0048	3.2
6	0198	0043	1.9	0133	0035	1.3	0259	0048	2.5	0145	0032	1.4
7	0126	0031	1.2	0074	0026	0.7	0145	0034	1.4	0056	0013	0.6
8	0084	0024	0.8	0039	0017	0.4	0078	0023	0.8	0037	0013	0.4
9	0059	0019	0.6	0029	0019	0.3	0042	0015	0.4	0027	0013	0.3
One-Wild (optimal = 1.1111)												
3	1.2785	0.0116	13.1	1.2781	0.0114	13.1	1.3414	0.0161	17.2	1.3413	0.0168	17.2
4	1.2946	0109	14.1	1.3105	0117	15.2	2709	0112	12.6	1.2630	0105	12.0
5	1.3714	0137	19.0	1.4125	0159	21.3	2775	0104	13.0	1.2828	0102	13.4
6	1.4990	0189	25.9	1.5948	0246	30.3	3257	0115	16.2	1.3794	0141	19.4
7	1.6793	0253	33.8	1.8333	0332	39.4	4196	0163	21.7	1.5757	0242	29.5
8	1.9034	0331	41.6	2.1332	0445	47.9	5621	0223	28.9	1.9037	0397	41.6
9	2.1590	0420	48.5	2.4703	0580	55.0	7562	0301	36.1	2.3703	0591	53.1
Slash (optimal = 5.9843)												
3	7.0895	0.2795	15.6	7.4991	0.3348	20.2	6.4815	0.2422	7.7	6.5367	0.2465	8.5
4	7.9896	3382	25.1	8.6854	0.4129	31.1	7.1538	.2796	16.3	7.6037	0.3339	21.3
5	8.9977	4355	33.5	10.819	0.9005	44.7	8.0679	3586	25.8	9.2930	0.7666	35.6
6	10.261	5815	41.7	14.567	1.4310	58.9	8.9836	4739	33.4	11.167	0.8863	46.4
7	11.487	7135	47.9	25.156	8.6783	76.2	10.555	7319	43.3	22.739	7.8504	73.7
8	12.692	8214	52.8	28.036	9.0950	78.6	11.705	5120	51.6	28.258	8.5066	78.8
9	13.999	9294	57.3	33.752	9.4908	82.3	12.908	6051	58.4	31.727	8.9310	81.1

several ampoules of n-Heptane material at NBS between May 22 and June 17, 1981. The ampoules were filled from two lots in several sets. Lot A includes 20 sets of ampoules; lot B includes six sets; only the data from 10 ampoules in sets from lot A will be used here. Panel A of table 5 shows the mean percent purity from 10 ampoules, where the mean was calculated as an average of anywhere between 5 and 10 measurements. To eliminate the big numbers and decimal points, we subtract 99.9900 and multiply by 10^4 in the third column.

Notice that, by virtue of the central limit theorem, one would expect that these averages would be approximately normally distributed and a higher value for the tuning constant, say $c = 5$, would be reasonable. The third column of Panel A reveals three somewhat anomolous values: -20, 56, and 28. Notice that the low value corresponds to ampoules in set 2, and the high value to those in set 20. Since the sets were filled sequentially, there may have been some aspect of the filling procedure

which caused these odd values. Also, the data are listed in the order in which they were measured, so the low value for the first ampoule may have resulted from some problem in the measuring equipment on the first day.

The iteration initiates with the median, $T^{(0)} = 7$, and s_{bi} is calculated from the median and 1.5 x MAD (= 12.0), yielding a scale estimate of 17.2. The convergence criterion in this calculation is relative to the estimated scale; i.e., the iteration ceases when either $k \geq 15$ or $|T^{(k)} - T^{(k-1)}|/s_{bi} \leq .0005$.

Panel B gives the bisquare weights associated with each observation and the biweight at each iteration. Notice that the three "suspect" values all receive lower weight than the other seven. The final scale estimate, 0.0019, is computed from the final location estimate, 99.9907, and the s_{bi} used throughout the iteration (.0017). These estimates compare favorably with the sample mean and standard deviation, 99.9910 and 0.0021.

TABLE 3. *Biweight variances and deficiencies: n=20.*

Tuning Constant	1.5xMAD — Fixed			1.5xMAD — Iterative			s_{bi} — Fixed			s_{bi} — Iterative		
	Variance	SE	Deficiency (%)	Variance	SE	Deficiency (%)	Variance	SE	Deficiency (%)	Variance	SE	Deficiency (%)
Gaussian (optimal = 1.0)												
3	1.0973	0.0076	8.8	1.0841	0.0069	7.8	1.2111	0.0147	17.4	1.2159	0.0154	17.8
4	.0369	0039	3.6	0299	0034	2.9	.0842	0064	7.8	0769	0051	7.1
5	0172	0026	1.7	0117	0013	1.2	0387	0036	3.7	0331	0024	3.2
6	0087	0015	0.9	0056	0007	0.6	0187	0019	1.8	0163	0015	1.6
7	0047	0008	0.5	0030	0004	0.3	0096	0010	0.9	0084	0008	0.8
8	0027	0005	0.3	0018	0002	0.2	0052	0005	0.5	0045	0004	0.4
9	0017	0003	0.2	0011	0001	0.1	0030	0003	0.3	0027	0002	0.3
One-Wild (optimal = 1.0526)												
3	1.1597	0.0077	9.2	1.1494	0.0055	8.4	1.2663	0.0148	16.9	1.2561	0.0139	16.2
4	1313	0040	7.0	1298	0037	6.8	1517	0066	8.6	1421	0053	7.8
5	1572	0049	9.0	1594	0050	9.2	1198	0034	6.0	1185	0034	5.9
6	2082	0069	12.9	2145	0071	13.3	1273	0037	6.6	1289	0037	6.8
7	2745	0094	17.4	2848	0097	18.1	1522	0047	8.6	1578	0050	9.1
8	3532	0122	22.2	3721	0127	23.2	1905	0062	11.6	2019	0067	12.4
9	4439	0151	27.1	4690	0159	28.3	2431	0081	15.3	2700	0092	17.1
Slash (optimal = 5.2666)												
3	6.2724	0.2046	16.0	6.4046	0.2284	17.8	5.6057	0.1410	6.1	6.7146	0.1541	7.8
4	7.5085	3189	29.9	8.1706	0.4386	35.5	6.2212	1976	15.3	6.4293	0.2137	18.1
5	8.8490	4364	40.5	10.255	0.6849	48.6	7.3065	2822	27.9	8.3053	0.4552	36.6
6	10.157	5377	48.1	12.260	0.8502	57.0	8.6312	4237	39.0	10.434	0.6585	49.5
7	11.453	6307	54.0	13.964	1.0004	62.3	10.116	5670	47.9	12.580	0.8205	58.1
8	12.733	7235	58.6	15.762	1.1107	66.6	11.832	7166	55.4	15.324	1.0068	65.7
9	13.996	8083	62.3	17.100	1.1866	69.2	13.442	8405	60.8	18.235	1.1790	71.1

In this case, there is little difference between the two procedures, and either may be reported. Had there been a substantial difference, one would want to examine the data more closely to understand the reason. This is an important step in data analysis, and robust methods offer easy, objective procedures for making this comparison and illustrating possible anomolies in the data.

6. Conclusions

This paper establishes the variance of the biweight as a location estimator across three distributional situations, for small to moderate sample sizes. In terms of scaling, s_{bi} performs more satisfactorily than does 1.5 x MAD, and need not be recalculated with subsequent iterations.

Three to six iterations of the w-iteration are typically required to attain satisfactory convergence ($< .0005$ x s_{bi}). The minimum efficiencies of the biweight across the three situations for sample sizes, 5, 10, and 20 at $c = 4$ are 46%, 83%, and 85% respectively; at $c = 6$ they are 33%, 67%, and 61% respectively. Gaussian efficiencies are considerably higher: at $c = 4$, 86%, 91%, and 92%; at $c = 6$, 94%, 97%, and 98%.

A final comment concerns the results on $n = 5$. For such a small sample size, it is encouraging that the biweight ($c = 4$) is only 14% less efficient than the optimal sample mean if the underlying population is really Gaussian. In fact, s_{bi} can be very misleading in a small (between 2% and 5% for the situations listed here) but influential proportion of the time. Conditioning on some ancillary statistic, such as the average value of the weights, would undoubtedly increase the efficiency for all three situations when $n = 5$.

TABLE 4. *Number of samples (out of 1000 samples of size*
n=5/n=10/n=20) that did not converge (k > 15 and $|T^{(k+1)}| >$
.0005 × scale).

(Tuning Constant)	1.5xMAD FIXED	1.5xMAD ITERATIVE	s_{bi} FIXED	s_{bi} ITERATIVE
Gaussian				
3	6/0/0	106/44/9	1/0/0	34/13/0
4	9/0/0	92/ 5/1	1/0/0	0/ 6/1
5	1/0/0	68/ 8/2	1/0/0	0/ 2/0
6	5/0/0	50/ 4/0	0/0/0	0/ 2/0
7	3/0/0	33/ 2/0	1/0/0	0/ 0/0
8	2/0/0	29/ 2/0	0/0/0	0/ 0/0
9	0/0/0	20/ 2/0	0/0/0	0/ 0/0
One-Wild				
3	3/0/0	120/ 11/ 6	0/0/0	18/13/ 0
4	1/0/0	168/ 14/ 3	0/0/0	0/10/ 3
5	1/0/0	170/ 42/ 0	0/0/0	0/ 9/ 0
6	0/0/0	159/ 70/ 3	0/0/0	0/47/ 0
7	1/0/0	138/ 91/ 6	0/0/0	0/46/ 0
8	0/0/0	121/113/20	0/0/0	0/36/ 0
9	0/0/0	92/120/37	0/0/0	0/22/32
Slash				
3	4/0/0	119/31/20	1/0/0	0/ 0/15
4	5/0/0	156/33/16	0/0/0	1/ 3/15
5	1/0/0	138/51/24	0/0/0	0/ 0/41
6	8/0/0	121/81/36	1/0/0	0/ 0/94
7	1/0/0	99/65/39	1/0/0	0/ 0/56
8	0/0/0	79/64/48	0/0/0	0/ 0/76
9	0/0/0	67/53/53	0/0/0	0/32/74
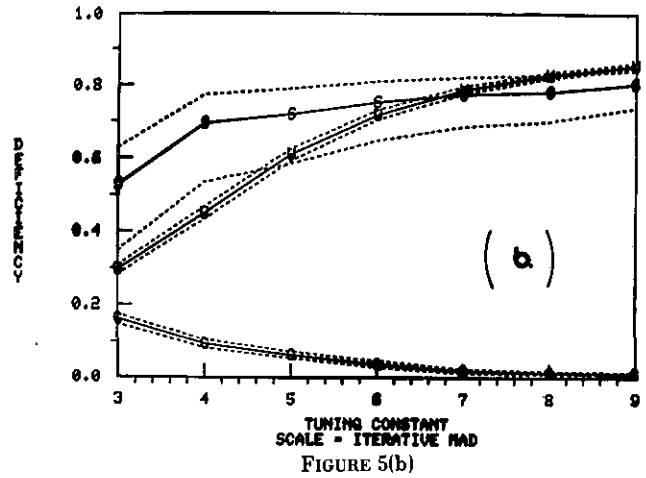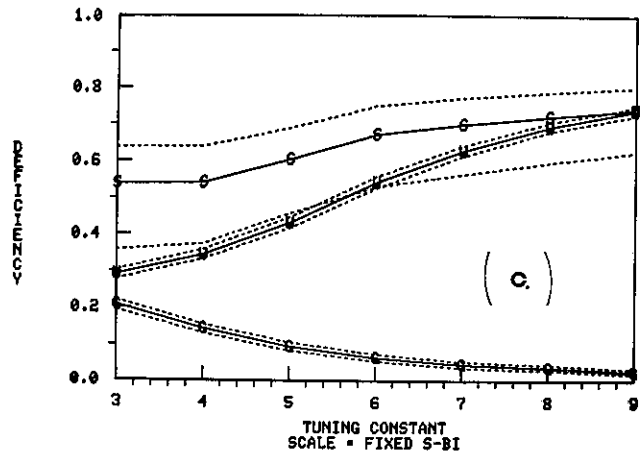
FIGURE 5(b)

FIGURE 5(c)

FIGURE 5(a)

FIGURE 5(d)

113

DEFICIENCIES OF BIWEIGHT,   N = 10

C = TUNING CONSTANT
SCALE = FIXED MAD
G = GAUSSIAN   W = ONE-WILD   S = SLASH
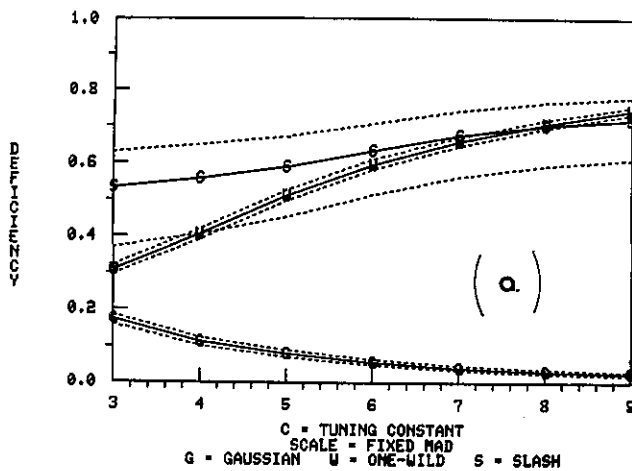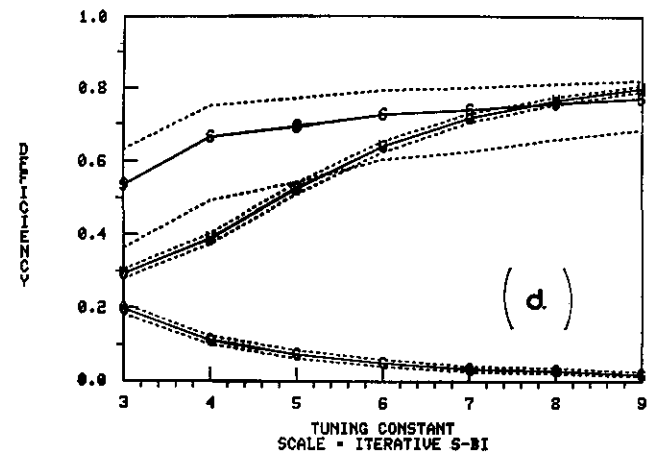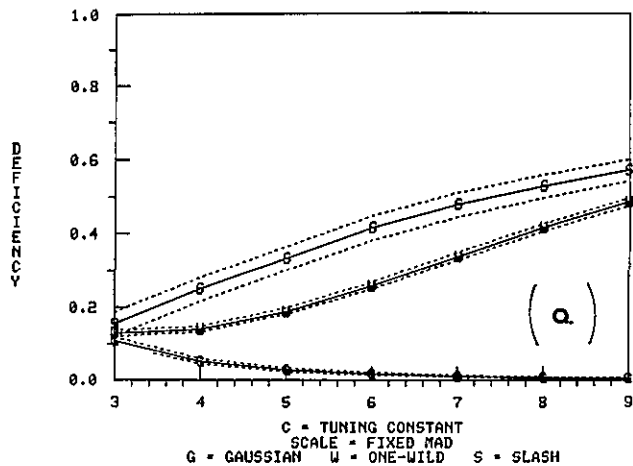
FIGURE 6(a)

DEFICIENCIES OF BIWEIGHT,   N = 10

C = TUNING CONSTANT
SCALE = ITERATIVE S-BI
G = GAUSSIAN   W = ONE-WILD   S = SLASH
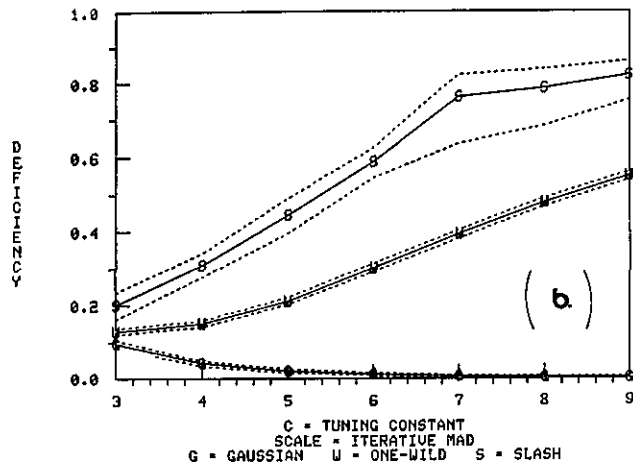
FIGURE 6(b)

DEFICIENCIES OF BIWEIGHT,   N = 10

C = TUNING CONSTANT
SCALE = FIXED S-BI
G = GAUSSIAN   W = ONE-WILD   S = SLASH
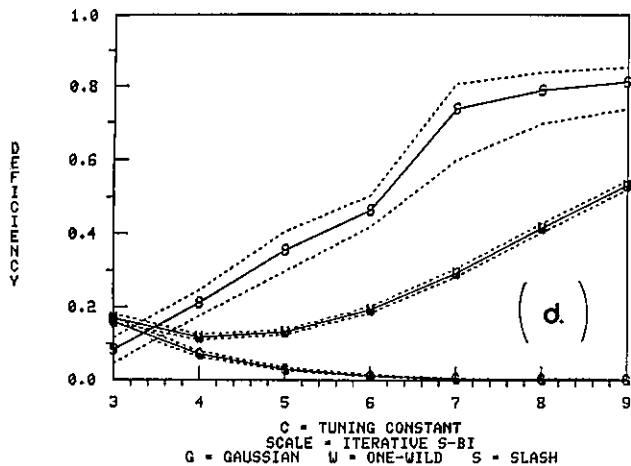
FIGURE 6(c)

DEFICIENCIES OF BIWEIGHT,   N = 10

C = TUNING CONSTANT
SCALE = ITERATIVE MAD
G = GAUSSIAN   W = ONE-WILD   S = SLASH

FIGURE 6(d)

DEFICIENCIES OF BIWEIGHT,   N = 20

C = TUNING CONSTANT
SCALE = FIXED MAD
G = GAUSSIAN   W = ONE-WILD   S = SLASH

FIGURE 7(a)

DEFICIENCIES OF BIWEIGHT,   N = 20

C = TUNING CONSTANT
SCALE = ITERATIVE MAD
G = GAUSSIAN   W = ONE-WILD   S = SLASH
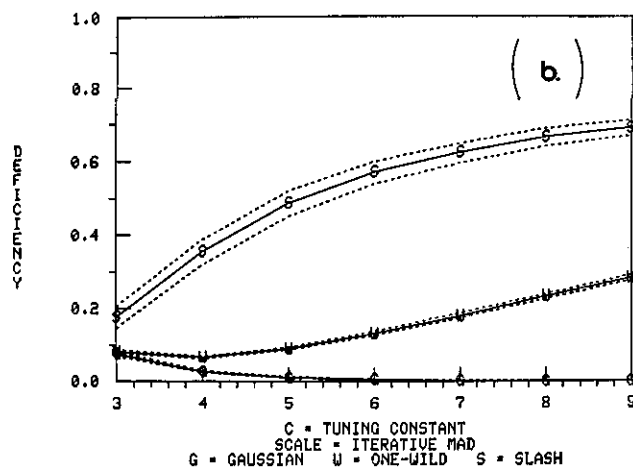
FIGURE 7(b)

DEFICIENCIES OF BIWEIGHT, N = 20

FIGURE 7(c)

DEFICIENCIES OF BIWEIGHT, N = 20
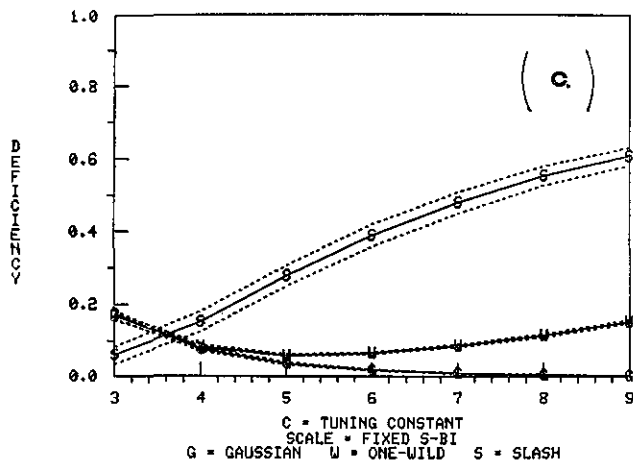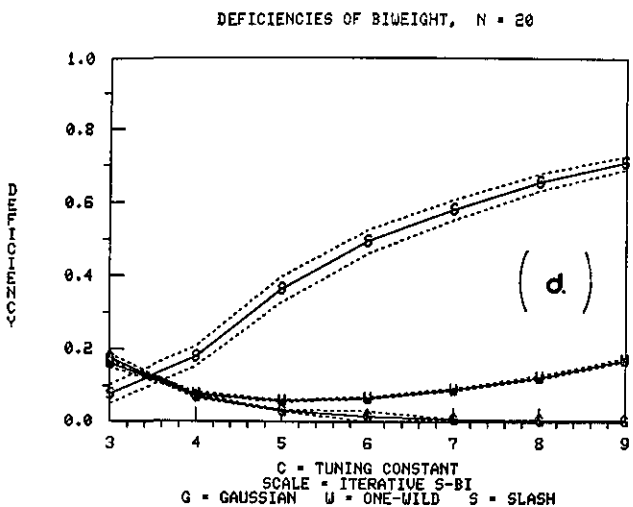
FIGURE 7(d)

7. References

[1] Andrews, D.F.; Bickel, P.J.; Hampel, F.R.; Huber, P.J.; Rogers, W.H.; and Tukey, J.W. (1972). *Robust Estimates of Location: Survey and Advances*, Princeton University Press: Princeton, New Jersey.

[2] Gross, A.M., and Tukey, J. W. The estimators of the Princeton Robustness Study. Technical Report No. **38**, Series 2, Department of Statistics, Princeton University, Princeton, New Jersey.

[3] Beaton, A.E., and Tukey, J.W. (1974). The fitting of power series, meaning polynomials, illustrated on band-spectroscopic data. Technometrics **16**, 147-185.

[4] Gross, Alan M. (1976). Confidence interval robustness with long-tailed symmetric distributions. J. Amer. Statist. Assoc. **71**, 409-417.

[5] Gross, Alan M. (1977). Confidence intervals for bisquare regression estimates. J. Amer. Stat. Assoc. **72**, 341-354.

[6] Kafadar, K. (1982b). Using biweights in the two-sample problem. Comm. Statist. **11**(17), 1883-1901.

[7] Tukey, J.W. (1960). A survey of sampling from contaminated distributions. In *Contributions to Probability and Statistics*, I. Olkin, ed., Stanford University Press, Stanford, California.

[8] Huber, P. (1981). *Robust Statistics*. Wiley: New York.

[9] Huber, P. (1964). Robust estimation of a location parameter. Ann. Math. Statist. **35**, 73-101.

[10] Lax, D. (1975). An interim report of a Monte Carlo study of robust estimates of width. Technical Report No. **93**, Series 2, Department of Statistics, Princeton University, Princeton, New Jersey.

TABLE 5. *Measurements on ampoules of n-Heptane.*

A) The data

Set No.–Ampoule	% purity	(% purity−99.99)·10^4
2-05	99.9880	−20
3-04	99.9909	9
20-20	99.9956	56
7-07	99.9908	8
20-03	99.9901	1
14-10	99.9928	28
2-15	99.9915	15
8-14	99.9899	− 1
14-20	99.9906	6
7-17	99.9894	− 6

B) Biweight iterations: $c=5$, $T^{(0)}=7.0$, $s^{(0)}=12.0$, $s_{bi}=17.2$

Columns give weights $w_i^{(k)}$ corresponding to each observation y_i at k^{th} iteration. $T^{(k)} = \Sigma w_i^{(k)} y_i / \Sigma w_i^{(k)}$

obsv'n	(1)	(2)	(3)	(4)	(5)
−20	.8120	.8082	.8075	.8074	.8074
9	.9989	.9992	.9992	.9993	.9993
56	.4546	.4597	.4606	.4607	.4608
8	.9997	.9999	.9999	.9999	.9999
1	.9903	.9893	.9891	.9891	.9891
28	.8839	.8869	.8875	.8876	.8876
15	.9827	.9839	.9841	.9842	.9842
− 1	.9827	.9815	.9812	.9812	.9812
6	.9997	.9996	.9995	.9995	.9995
− 6	.9547	.9527	.9523	.9523	.9523

$$T^{(1)}=7.283 \quad T^{(2)}=7.334 \quad T^{(3)}=7.344 \quad T^{(4)}=7.345 \quad T^{(5)}=7.346$$
$$s_{bi}=18.648$$

Final location and scale estimates (original scale):

$$\hat{\mu} = 99.9900 + 7.346/10^4 = 99.9907$$
$$\hat{\sigma} = 18.648/10^4 = .0019$$

[11] Tukey, J.W.; Braun, H.I., and Schwarzchild, M. (1977). Further progress on robust/resistant widths. Technical Report No. 129, Series 2, Department of Statistics, Princeton University, Princeton, New Jersey.

[12] Simon, G. (1976). Computer simulation swindles with applications to estimates of location and dispersion. Appl. Statist. 25, 266-274.

[13] Tukey, J.W. (1977). Lecture Notes to Statistics 411. Unpublished manuscript, Princeton University, Princeton, New Jersey.

[14] Rogers, W.F., and Tukey, J.W. (1972). Understanding some long-tailed symmetrical distributions. Statistica Neerlandica 26, No. 3, 211-226.

[15] Kafadar, K. (1982a). A biweight approach to the one-sample problem. J. Amer. Stat. Assoc. 77, 416-424.

[16] Kronmal, J. (1964). Evaluation of the pseudorandom number generator. J. Assoc. Computing Machinery, 351-363.

[17] Box, G.E.P., and Muller, M. (1958). A note on generation of normal deviates. Ann. Math. Stat. 28, 610-611.

[18] Mosteller, F., and Tukey, J.W. (1977). *Data Analysis and Regression: A Second Course in Statistics*. Addison-Wesley; Reading, Massachusetts.

[19] Holland, P.W., and Welsch, R.E. (1977). Robust regression using iteratively reweighted least squares. Comm. Statist. A6(9), 813-827.

High Precision Coulometric Titration of Uranium

George Marinenko, William F. Koch, and Edgar S. Etz*

National Bureau of Standards, Washington, DC 20234

An improved method for the coulometric assay of uranium and uranium oxide has been developed based on the electrogeneration of Ti(III) in H_2SO_4, using Fe(II) as a catalyst. The endpoint is determined amperometrically. Hydrogen peroxide is used as the oxidant in the dissolution of the uranium to avoid interferences from nitrate. The precision of the method as indicated by the standard deviation of an individual observation ranged from 0.008 weight percent for the analysis of the metal to 0.02 weight percent for the analysis of the oxides.

Key words: amperometry; coulometric titration; electrogeneration; high-precision coulometry; hydrogen peroxide; standard reference material; titanium; titanous ion; uranium; uranium oxide.

1. Introduction

Coulometry is an absolute method of analysis based on Faraday's Laws of Electrolysis which relate electric current (i), time (t), and chemical equivalent weight (mole) through the equation:

$$\text{mole} = \frac{1}{F} \int_0^t i \, dt.$$

The constant of proportionality, F, is the Faraday, the exact value of which has been the subject of intense research over the years at the National Bureau of Standards (NBS) [1-4][1]. The parameters which define the analytical system are based on measurements of physical quantities, the national standards of which are maintained by NBS, i.e., volt, ohm, second, and gram.

This paper is another from a series of investigations designed to develop highly precise and accurate analytical procedures based upon the coulometric technique. Earlier papers have described the coulometric titrations of acids and bases [5], halides [6], and potassium dichromate [7]. The method described here has been developed for high-precision analysis of uranium metal and its compounds, which are of great scientific, industrial, and commercial importance. Some portions of this investigation have been previously reported at the 1965 EURATOM Conference

on High Precision Analysis of Substances of Interest to Nuclear Energy [8].

Among the multitude of existing methods for analysis of uranium, only a few are sufficiently precise for assaying relatively high purity materials. The classical methods involve preliminary reduction of uranyl ion to a mixture of tri- and tetravalent uranium by either passing it through a Jones reductor or reducing the uranyl ion at a mercury or gold amalgam cathode, followed by air oxidation of U(III) to U(IV) and finally oxidation of U(IV) to U(VI) with an oxidant such as $K_2Cr_2O_7$ [9,10]. One variation involves potentiometric titration of a mixture of trivalent and tetravalent uranium (obtained from a Jones reductor) first to U(III) – U(IV) endpoint and then to U(IV) – U(VI) endpoint. The uranium content is calculated from the difference between the two endpoints [11]. In another variation, U(III) – U(IV) mixture is titrated potentiometrically to the first endpoint, then solid dichromate is added in excess and the excess dichromate is determined coulometrically [12]. Another method involves the dissolution of uranium metal in orthophosphoric acid, followed by a titration with dichromate using no prereduction [13]. Recently a precise titrimetric method for uranium was reported by Leon Pszonicki [14]. In this method U(VI) is reduced to U(III) in hydrochloric acid solution, using an amalgamated cadmium reductor. Orthophosphoric acid is used to oxidize U(III) to U(IV) followed by quantitative oxidation with dichromate to U(VI). All of the aforementioned procedures involve the use of potassium dichromate as the quantitative oxidant converting U(IV) to U(VI). Most require pre-reduction

and pre-titration steps to prepare the analyte for the actual assay.

An alternative to the oxidative assay of U(IV) to U(VI) is one based on a quantifiable reduction of U(VI) to U(IV). Such a procedure requires a strong reductant obtainable in a purified and stable form and deliverable in discrete quantities during the course of a titration. Of the possible chemical species meeting these requirements, titanous ion (Ti(III)) has proved to be the reductant of choice for this application. Several articles have been written describing conditions for the generation of Ti(III) [15-17]. The first successful coulometric titration method for uranium with the use of electrogenerated Ti(III) was reported by Lingane and Iwamoto [18]. This method uses a mercury-pool cathode at elevated temperatures to effect complete and efficient reaction.

Kennedy and Lingane proposed another coulometric procedure employing a platinum cathode and a catalyst. Their procedure was intended to circumvent the drawbacks associated with a mercury cathode and high temperatures [19,20]. In the present paper, a method based on the work of Kennedy and Lingane is described. The existing procedure has been refined to improve the precision and accuracy of the assay of uranium and to make it applicable to the certification of Standard Reference Materials (SRMs).

2. Summary of Method

The method is based on the coulometric reduction of hexavalent uranium, U(VI), to the tetravalent state, U(IV), using titanous ion, Ti(III), as the intermediate reductant and Fe(II) as a catalyst. This reduction takes place in a solution of 1 mol/L titanyl sulfate and 9 mol/L sulfuric acid at a platinum cathode in the controlled-current mode. The current density of the cathode is maintained at or below 2.5 mA/cm². The standard potentials of the reduction reactions are:

$$UO_2^{2+} + 4H^+ + 2e = U^{4+} + 2H_2O \quad E^0 = +0.334$$

$$TiO^{2+} + 2H^+ + e = Ti^{3+} + H_2O \quad E^0 = +0.1$$

$$Fe^{3+} + e = Fe^{2+} \quad E^0 = +0.771 .$$
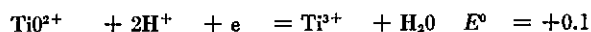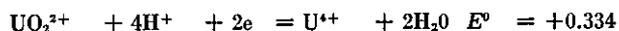
At the beginning of the titration, direct reduction of U(VI) to U(IV) is the principal cathodic reaction. As the uranyl ion concentration is depleted, coreduction of titanyl ion begins. The generated titanous ion in turn acts as a reductant for the remaining uranyl ion in the bulk of the solution. Finally, as the endpoint is approached, titanous ion generation becomes the principal cathodic reaction. Under these conditions, the overall reduction of U(VI) to U(IV) occurs with 100 percent current efficiency.

To add further complexity to the reduction process, it has been reported by various authors, and verified in our laboratory, that the rate of reduction of U(VI) by Ti(III) is a slow process. Lingane and Kennedy [19] pointed out that in a sulfuric acid medium the reduction of U(VI) to U(V) proceeds rapidly, but further reduction to U(IV) is the slow and rate-determining step. They found that small amounts of ferrous ion catalyze the reduction of U(V) to U(IV) facilitating the titration at room temperature. Ferrous ion reduces U(V) to U(IV) more rapidly than does Ti(III) and in turn the ferric ion produced in this reaction is reduced relatively rapidly by the trivalent titanium.

Unfortunately, even in the presence of ferrous ion, the kinetics of this reaction are not sufficiently favorable for high precision work. The approach to equilibrium is slow. The rate expression derived by Kennedy and Lingane for this reaction in a sulfuric acid medium is:

$$\frac{-d\,[Ti(III)]}{dt} = k\,\frac{[Ti(III)]^2}{[Ti(IV)]}\,\frac{[U(VI)]}{[H_2SO_4]} .$$

It is apparent that since the rate of the reaction is of the first order with respect to U(VI) concentration and of the second order with respect to Ti(III) concentration, the equilibrium is established more rapidly in the presence of excess Ti(III). Accordingly, it is advantageous to over-titrate by generating a slight excess of Ti(III) and then, when equilibrium is established, to extrapolate back to the equivalence point after determining the response factor of the indicator electrode.

The principal modifications to the method which are described in the paper and which have resulted in increased precision and accuracy are:

- a more stable endpoint detection system composed of a platinum versus saturated calomel electrode pair in the amperometric mode, rather than the dual platinum biamperometric technique;
- highly stable and accurate current-controllers and timing circuitry to assure accurate integration of charge;
- improved dissolution procedures for uranium metal and oxides;
- overtitration to improve the kinetics at the endpoint.

3. Experimental

3.1 Apparatus

The apparatus used in this work is described in detail in previous publications [2,21-24]. The constant-current sources are of two types. The first employs a commercially-available power supply operated in the

118

constant-current mode. The instrument has a maximum output of 60 V and a current rating of 0 to 2 A. The stability of this power supply is on the order of 0.001 percent per 8 hours and its reliability proven through its use in high-precision coulometric iodimetry [21] and on the determinations of the atomic weights of gallium [22] and zinc [23]. The second type of current-source, used in the later stages of this experiment, was designed and built at NBS in connection with a redetermination of the Faraday via 4-aminopyridine [24]. It is powered by batteries to minimize problems associated with ac ripple and ground loops and is stable to better than 0.001 percent per 8 hours.

The output of either current source is adjusted such that the current flowing through a standard resistor (which is in series with the coulometric titration cell) produces a potential equal to the emf of a Weston saturated cell. Balance is monitored with a null-point detector such as a microvoltmeter or galvanometer, and maintained manually.

The standard resistors are of the NBS-type, devoid of their metal containers and immersed in a large oil-bath to ensure temperature stability. The Weston saturated cells were enclosed in a thermostated box. The cells and resistors are periodically calibrated against the national working standards of voltage and resistance maintained at NBS. A commercially available electronic frequency meter was used as the timer, its operational mode set to count the cycles of the NBS 10 kHz standard frequency. The current-source and timer are integrated through a switching system, designed and built at NBS. In the standby position, the current flows through a surrogate load resistor comparable in resistance to that of the titration cell, and the timer gate is open; in the active position, the current is channeled to the titration cell, and the timer gate is closed.

The titration cell, similar to one used in previous high-precision coulometric research at NBS [2], is constructed of two 180 mL tall-form beakers connected by two intermediate chambers with fritted-glass separaters. A silicic acid gel plug was prepared in the last compartment of the titration H-cell by mixing sodium silicate solution with sulfuric acid directly in the compartment. The volumes of solutions used in gel preparation were selected such that the amount of gel produced would fill one-half of the 180 mL beaker, completely covering the glass frit of the connecting chamber. Sulfuric acid (2 mol/L) was poured over the silicic acid plug. The titration cell was further extended through a U tube, containing another silicic acid plug, to a 180 mL beaker filled with saturated KCl solution and serving as the anode compartment. The saturated calomel reference electrode of the indicator circuit was also dipped into this compartment.

A modified cage-type platinum electrode was used as the cathode. It consisted of a platinum foil cylinder concentrically located within a platinum strip cage. The apparent area of the former was 28 cm^2, and of the latter 12 cm^2, yielding a total area of 40 cm^2. Early experiments showed that the platinum cathode will perform less than satisfactorily if its surface is not properly prepared. Consequently the conditioning procedure described below was scrupulously followed:

a) store the electrode each night in a solution of 1 mol/L $K_2Cr_2O_7$ and 2 mol/L H_2SO_4

b) rinse with distilled water and soak in a solution of 0.1 mol/L ferrous ammonium sulfate and 2 mol/L H_2SO_4

c) rinse thoroughly with distilled water and install in titration cell.

After several titrations, it was sometimes necessary to strip the surface of the electrode by dipping it in aqua regia for 5 minutes and then reconditioning it according to the above procedure. The anode was a silver cylinder made from 2 mm thick foil and having a surface area of 100 cm^2.

The amperometric indicator system consisted of a platinum foil electrode (1 cm^2) and a saturated calomel electrode (SCE) with a flushable liquid junction. A polarograph was used as the source of the applied emf as well as for recording the indicator current. The value of applied emf was determined by running a current-voltage scan using the indicator electrode versus the SCE in the titration cell containing a solution similar to that expected at the equivalence point of an actual titration (Figure 1). The flat portion of this voltammogram typically extended from about +0.2 to +0.3 V versus SCE, which represents the useable window for the applied emf. Since this window is rather narrow (due to the oxidation of Fe(II) at voltages more positive than +0.3 V and the reduction of Ti(IV) at voltages below +0.2 V) and has a tendency to shift slightly from titration to titration, it is important that the potentiostat of the polarograph be very stable to achieve linearity in the endpoint current readings.

All weighings were performed on a 20 g capacity microbalance and were precise to 0.003 mg. The weights of all samples were corrected for air buoyancy.

Either nitrogen or argon was passed through the supporting electrolyte prior to and during the titration to keep atmospheric oxygen out of the cell. This purging gas was purified and conditioned by bubbling it through a chromous sulfate solution and then through a tower containing 9 mol/L H_2SO_4.
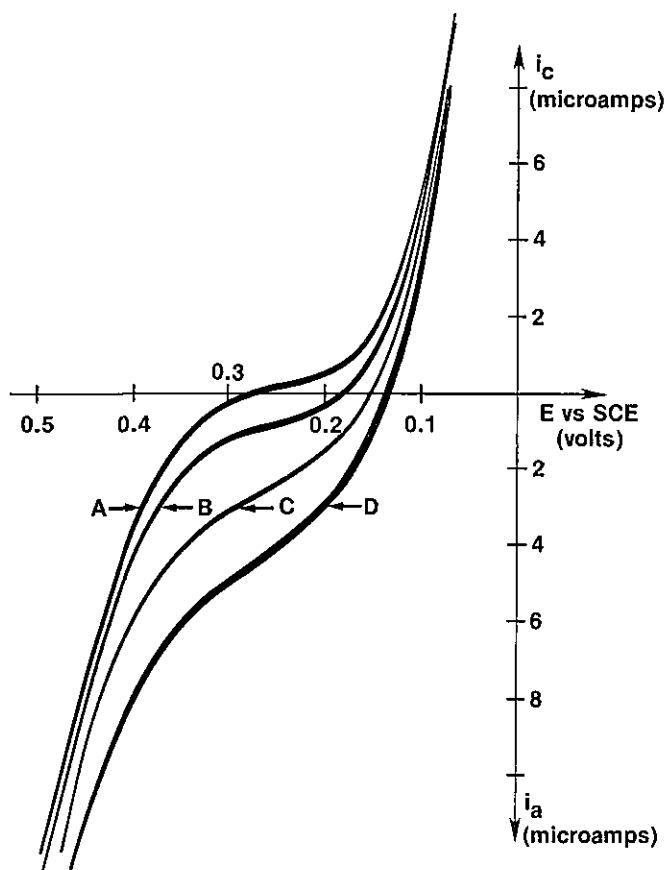
FIGURE 1. Current-voltage curves. Platinum indicator electrode vs. SCE reference electrode in coulometric titration cell. Supporting electrolyte: 9 mol/L H_2SO_4, 1 mol/L Ti(IV), 0.1 g $Fe(NH_4)_2(SO_4)_2$, 100 μeq U. (A) at endpoint. (B) 20 μeq excess of Ti(III). (C) 50 μeq excess of Ti(III). (D) 80 μeq excess of Ti(III).

3.2 Reagents

The uranium which was assayed in this work was of two forms: the pure metal cast in dingots, one lot of which became Standard Reference Material 960; and the oxide of uranium of nominal stoichiometry U_3O_8 including samples of SRM 950a and SRM 950b.

The supporting electrolyte in the cathode compartment was a solution of 9 mol/L sulfuric acid and 1 mol/L titanyl sulfate. It was prepared according to the following procedure: purified liquid titanium tetrachloride is partially hydrolyzed (50% by weight) by slowly adding it to distilled water which is being well stirred and cooled in an ice-bath. The reaction is vigorous and exothermic. It must be carried out in a fume hood, because hydrogen chloride gas is liberated. The resulting solution is approximately 2.6 molal Ti(IV). This hydrolyzed titanium solution is then added slowly to concentrated (95%) sulfuric acid (ACS reagent-grade) (750 g Ti(IV) solution per liter of sulfuric

acid). Once again HCl is evolved rather vigorously. When addition is complete, the solution is purged with nitrogen to remove all traces of HCl. A clear solution should result. Dilute with distilled water such that the final solution is 9 mol/L H_2SO_4 and 1 mol/L Ti(IV). [Note: After several weeks, a white precipitate of TiO_2 will form due to the hydrolysis of the titanyl sulfate. Since this effectively depletes the Ti(IV) available for reaction, the solution should be discarded and fresh electrolyte prepared.]

The acids and the hydrogen peroxide used in the dissolution of uranium were ACS-reagent grade, as was the ferrous ammonium sulfate hexahydrate used to catalyze the reduction of U(VI).

3.3 Preparation and Dissolution of Uranium Metal

Using bolt-cutters, the dingot is cut into pieces weighing approximately 1 gram each. Surface oxide and impurities are removed by dipping the uranium sample in 8 mol/L HNO_3 for 10 minutes, rinsing in distilled water, etching in 3 mol/L HCl for 5 minutes, rinsing in distilled water, and drying in a vacuum desiccator. The sample is weighed on a calibrated analytical balance before the oxide reappears, correcting for the buoyancy of air (density of uranium, 19.05 g/cm³). The sample is placed into a 125 mL Erlenmeyer flask and dissolved slowly in 2-10 mL of 6 mol/L HCl, warming if necessary on a hot plate. It has been found most convenient to rest the flask in an inclined position in a small crystallizing dish throughout the dissolution process. An inverted 50 mL beaker is placed over the top of the flask to catch any possible spattering. After the metal has dissolved and only a small amount of black residue remains, 2 mL of 16 mol/L HNO_3 are slowly added to oxidize all of the uranium to the hexavalent state, U(VI). The black residue will also dissolve. The beaker serving as the splash guard is rinsed with 5 mL of distilled water, this water being added to the sample flask. The walls of the flask are then rinsed with 5 mL of distilled water. Next, 5 mL of concentrated H_2SO_4 (95%) are carefully added to the sample. The solution is then evaporated down to SO_3 fumes three times with the addition of 5 mL of water after each fuming. It is imperative that all traces of chloride and nitrate be removed from the solution. (Nitrate is reduced at the cathode and as such would pose a serious interference in the subsequent coulometric titration.)

To avoid the repetitive fumings required to eliminate nitrate, hydrogen peroxide can be used instead of nitric acid to oxidize the uranium. With this procedure, after the metal has dissolved in HCl, 1 mL of H_2O_2 (30%) is added slowly. A light yellow precipitate (a peroxide of uranium) may form but is unstable and is rapidly reduced back to U(VI) upon heating, resulting in a clear brilliant yellow solution. To destroy the excess hydrogen

peroxide the solution is evaporated nearly to dryness. The sides of the flask are then rinsed with distilled water and 5 mL of H_2SO_4 (95%) are added to the solution. The solution is then evaporated to SO_3 fumes. If allowed to stand a day or two, a crystalline percipitate may appear. Distilled water should be added to redissolve the precipitate, with subsequent evaporation to SO_3 fumes again before analyzing.

Blanks containing the same volumes of reagents used in the dissolution of the uranium samples were put through the same evaporation procedure. To some of these blank samples were added 30.31 μeq of uranium from a stock solution.

3.4 Preparation and Dissolution of Uranium Oxide (U_3O_8)

A sample of the uranium oxide (approximately 1.5 g) is placed in a platinum boat and ignited in a furnace for 1 hour at 900 °C (SRM 950b was fired at 800 °C). After the firing process, the sample is allowed to cool for 15 minutes, and stored in a desiccator. After cooling, the boat plus sample is weighed on a calibrated analytical balance, the sample is dumped from the boat into a 125 mL Erlenmeyer flask, and the empty boat is reweighed. The mass of the sample is calculated by difference, corrected for the buoyancy of air (density of uranium oxide 8.3 g/cm^3). The sample is digested in 10 mL of 12 mol/L HCl on a warm hotplate overnight (8 to 12 hours). Care should be taken to avoid evaporating the solution to dryness. As described earlier, the flask is in an inclined position with a beaker over the top. After the uranium oxide sample is dissolved (some black residue may remain), the sample is carried through the oxidation and fuing procedures outlined in section 3.3. Either nitric acid or hydrogen perioxide may be used, with the latter being preferred.

3.5 Coulometric Titration

Prior to delivery of the sample, 75 mL of supporting electrolyte are added to the cathode chamber of the cell togetehr with 100 mg of ferrous ammonium sulfate hexahydrate. Nitrogen or argon is then passed through the compartment and into the chamber for one-half hour to remove air. After purging, the catholyte is permitted to flow into the intermediate compartments to the extent that it just covers the bottom of each compartment, thus establishing electrolytic connection between the anode and cathode chambers.

A small amount of uranyl sulfate solution, about 5μeq, is then added to the cathode chamber and is pre-titrated by passage of small increments of charge equivalent to 1 μeq using 3-10 mA. At the conclusion of each increment,

the amperometric indicator current is recorded. This current, small and essentially constant up to the equivalence point, exhibits a curvature in the vicinity of the equivalence point and becomes a linear function of the concentration beyond the equivalence point. After the first excess of Ti(III) is noted, the solution is permitted to equilibrate for one-half hour, after which increment-wise generation is resumed. The linear portion of the indicator current is extrapolated graphically and its intersection with the zero-current line is taken as the endpoint.

After completion of the pre-titration, the intermediate cell chambers are rinsed by repeatedly emptying and filling the chambers with electrolyte, applying suction or nitrogen pressure as required. The final reading of the indicator current is recorded and this reading is used to determine the amount of overtitration of the pre-titration step.

Following the pre-titration, the intermediate compartments are completely filled with catholyte and the sample, which has been deaerated, is delivered into the cathode chamber by applying nitrogen pressure to a specially designed polyethylene siphon system.

The sample is titrated using 101 mA current for a precalculated period of time corresponding to a few microequivalents in excess of the stoichiometric amount. The middle compartments are again emptied into the cathode chamber using nitrogen pressure. The sample flask, which is still connected to the cathode chamber through the siphone tube, is rinsed several times with the catholyte by alternately applying vacuum and pressure to the siphon system.

Following the one-half hour equilibration period, small increments of charge are again passed as already described in the pre-titration procedure and the indicator current is recorded after each addition. The indicator current curve is again extrapolated to locate the virtual endpoint. The charge required to reduce the uranium is the amount to the endpoint plus the excess resulting from the preceding pre-titration.

4. Results and Discussion

As in any precise chemical analysis, it was necessary to determine the blank resulting from reagents used in the sample preparation. It is quite apparent that any of the ions which are reducible by Ti(III) will be titrated along with uranium, yielding high results. It should be noted, however, that reducible impurities in the supporting electrolyte do not contribute to the overall blank since they are removed in the pre-titration step.

To evaluate the bias arising from chemical treatment of the sample, a number of titrations were made of samples containing 30.31 μeq of uranium which had been

processed with the same quantities of acids as in the larger sample preparation. The results for titrations of 11 aliquot samples gave a blank value of $+0.27$ μeq $\pm$ 0.17 μeq. In addition, a study was made of the relationship between the sample size and the assay. This study indicated a systematic increase of the assay value as the sample size decreased. The plot of the difference between the calculated and found number of equivalents verses sample size for 30 determinations of the uranium content in dingot metal yields a linear relationship that, upon extrapolation to zero sample size, gives an intercept close to 0.35 μeq (Fig. 2), well within the uncertainty of the value obtained in the blank titrations. On the basis of these two pieces of experimental evidence, a 0.27 μeq bias must be subtracted from all titrations.
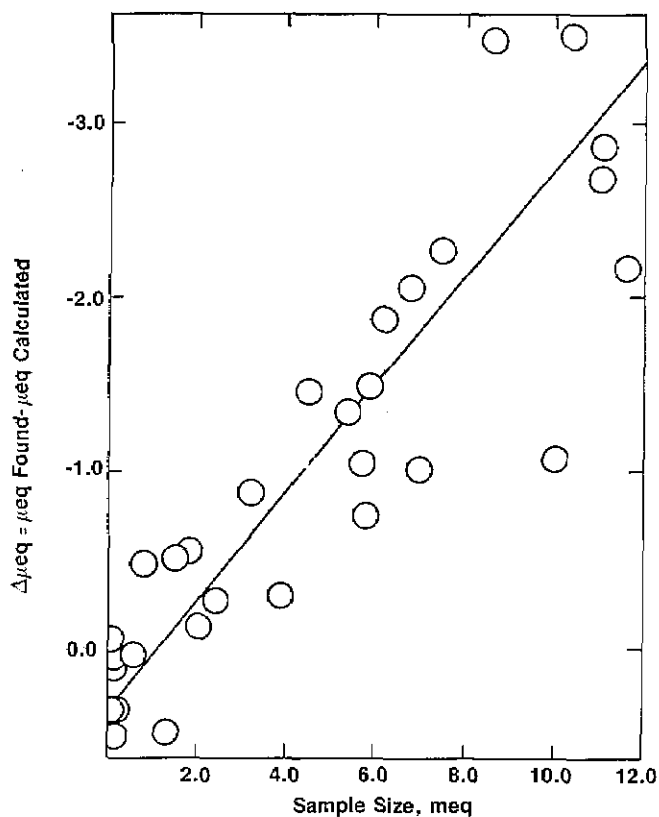
FIGURE 2. Analysis of titration data for bias.

A summary of the titration data of dingot uranium, corrected for the bias, is given in Table 1. The data were subdivided into four groups, encompassing different sample sizes: Group I — up to 100 mg of U; Group II — 100 to 500 mg of U; Group III — 500 to 100 mg of U; and Group IV — higher than 1000 mg of U. The table summarizes individual results, along with the respective averages, and the corresponding standard deviation of a single determination for each group. It

TABLE 1. *Assay in weight percent, of dingot uranium in method development.*

| | Average Sample, Size, mg | | |
50	300	750	1010
100.18	99.966	99.964	99.964
100.15	99.957	99.954	99.979
99.31	99.977	99.977	99.972
99.95	99.970	99.964	99.973
99.88	99.966	99.980	99.987
100.18	99.971	99.948	
99.91	99.982	99.985	
99.96	99.982	99.962	
	99.978	99.947	
	99.983	99.984	
	99.974	99.976	
	99.968	99.974	
	99.975	99.993	
	99.969		
	99.965		
	99.982		
Average			
99.94	99.973	99.970	99.975
Std. Dev.			
0.29	0.008	0.015	0.009

can be seen that for larger samples, the precision remains constant.

It should be kept in mind that the assay reported here represents the reductometric value for the material, and as such would include iron and any other impurities in the uranium which would be reduced by trivalent titanium.

Uranium metal, issued by NBS as SRM 960, was analyzed independently by two analysts who used this method. The results are shown in table 2. Excellent agreement is obtained between the two analyses, indicating no operator bias. A correction of -0.0108 weight percent must be applied to this reductometric assay due to two electroactive impurities known to be present, 42.1 ppm iron and 4 ppm vandium. Thus this material is certified at 99.975 weight percent uranium.

TABLE 2. *Analysis of uranium metal, SRM 960. (uncorrected for impurities, see text)*

Analyst	Number of Determinations	Atomic Weight of Uranium in Sample	Assay Weight Percent	Standard Deviation
A	21	238.0289	99.9855	0.0081
B	4	238.0289	99.9848	0.0038

The developed method of analysis was also used for the assay of various U_3O_8 preparations. The values obtained for these materials are summarized in table 3. SRM 950a and SRM 950b are of natural uranium isotopic composition and are issued by NBS as chemical standards

TABLE 3. *Analysis of Uranium Oxide, U_3O_8.*

Material	Number of Determinations	Atomic Weight of Uranium in Sample	Assay Weight Percent	Standard Deviation
SRM	3	238.03	99.923	0.023
SRM 950b	6	238.03	99.958	0.022
Depleted				
Secondary	3	238.050	99.929	0.027
Depleted				
Primary	3	238.051	99.921	0.009
Enriched				
Primary	3	235.047	99.922	0.006

for uranium analyses. The other materials are for use in the preparation of uranium isotopic standards. The atomic weights were calculated from the isotopic abundances of uranium in the various samples. All of the materials were "pure" in that the total of metallic impurities did not exceed 0.01 percent.

5. Summary

An improved method for the coulometric assay of uranium and uranium oxide has been developed based on the electrogeneration of titanous ion in sulfuric acid. Ferrous ion is used as a catalyst. The endpoint using an amperometric system is determined by extrapolation after a slight overtitration which increases the reaction rate and guarantees complete reaction. Hydrogen peroxide is employed as the oxidant in the dissolution procedure in lieu of nitric acid which if not completely destroyed would greatly interfere with the subsequent coulometric titration. The method has been applied to the analysis of several preparations of uranium metal and uranium oxide, including SRM's. The demonstrated precision for the assay of the metal as represented by the standard deviation of the individual measurement ranges from 0.004 to 0.008 weight percent, and that for the assay of the oxide from 0.006 to 0.027 weight percent.

6. Acknowledgments

7. References

[1] Craig, D. N.; Hoffman, J. I.; Law, C. A. Hamer, W. J. Determination of the value of the Faraday with a silver-prechloric acid coulometer. J. Res. Natl. Bur. Stand. (U.S.). 64A(5): 381-402; 1960 September-October.

[2] Marinenko, G; Taylor, J. K. Electrochemical equivalents of benzoic acid and oxalic acid. Anal. Chem. 40(11), 1645-1651; 1968 September.

[3] Koch, W. F. The value of the Faraday via 4-aminopyridine. In *Atomic Masses and Fundamental Constants 6*, J. A. Nolen, Jr. and W. Benenson, ed. New York, NY: Plenum Publishing Corp.; 1980, 167-172.

[4] Bower, V. E.; Davis, R. S.; Murphy, T. J.; Paulsen, P. J.; Gramlich, J. W.; Powell, L. J. Recalculation of the Faraday constant due to a new value for the atomic weight of silver. J. Res. Natl. Bur. Stand. (U.S.). 87(1): 21-22; 1982 January-February.

[5] Taylor, J. K.; Smith, S. W. Precise coulometric titration of acids and bases. J. Res. Natl. Bur. Stand. (U.S.). 63A(2): 153-159; 1959 September-October.

[6] Marinenko, G.; Taylor, J. K. Precise coulometric titration of halides. J. Res. Natl. Bur. Stand. (U.S.). 67A(1): 31-35; 1963 January-February.

[7] Marinenko, G.; Taylor, J. K. Precise coulometric titrations of potassium dichromate. J. Res. Natl. Bur. Stand. (U.S.) 67A(5): 453-459; 1963 September-October.

[8] Taylor, J.K.; Marinenko, G. High-precision coulometric titrations with special reference to the determination of uranium. Proceedings of the conference on high-precision analysis of substances of interest to nuclear energy. EURATOM; Brussels, Belgium 1965. 147-153.

[9] Rodden, C. J.; Warf, J. C. Uranium, chapter 1 in *Analytical Chemistry of the Manhattan Project*. C. J. Rodden, ed. New York, NY: McGraw-Hill Book Company, Inc.; 1950. 3-159.

[10] Kramer, H. Determination of uranium with high precision, New Brunswick Laboratory Report; 1960, May. 20 p.

[11] Voss, F. S.; Green, R. E. A precision potentiometric titration method for the determination of uranium. Atomic Energy Commission (U.S.). AEC Report 4030; 1955. 11 p.

[12] Vita, O. A.; Trivisonno, C. F.; Walker, C. R. An improved titrimetric method for the precise determination of uranium. Goodyear Atomic Corp. Report. GAT-471 Chemistry; 1962 November. 10 p.

[13] Duckitt, J. A.; Goode, G. C. A method for high-precision assay of uranium metal. Analyst. 87(1031), 121-124; 1962 February.

[14] Pszonicki, L. Precise titrimetric determinations of uranium in high-purity uranium compounds. Talanta 13(3), 403-408; 1966 March.

[15] Arthur, P.; Donahue, J. F. Titanic chloride as an intermediate in coulometric analyses. Anal. Chem. 24(10), 1612-1614; 1952 October.

[16] Malmstadt, H. V.; Roberts, C. B. Automatic spectrophotometric titration with coulometrically generated titanous ion. Anal. Chem. 27(5), 741-744; 1955 May.

[17] Parsons, J. S.; Seaman, W. Coulometric titration of dyes with externally generated titanous ion. Anal. Chem. 27(2), 210-212; 1955 February.

[18] Lingane, J. J.; Iwamoto, R. T. Coulometric titration of uranium with electrogenerated titanous ion. Anal. Chim. Acta. 13(5), 465-472; 1955 November.

[19] Lingane, J. J.; Kennedy, J. H. Coulometric titration of iron, cerium and vanadium with titanous ion. Anal. Chim. Acta. 15(5), 465-472; 1956 November.

[20] Kennedy, J. H.; Lingane, J. J. Coulometric titration of uranium and uranium-vanadium mixtures with +3 titanium. Anal. Chim. Acta. 18(3), 240-244; 1958 March.

[21] Marinenko, G; Taylor, J. K. High-precision coulometric iodimetry. Anal. Chem. 39(13), 1568-1571; 1967 November.

[22] Marinenko, G. On the atommic weight of gallium. J. Res. Natl. Bur. Stand. (U.S.). 81A(1): 1-4; 1977 January-February.

[23] Marinenko, G. Absolute determination of the electrochemical equivalent and the atomic weight of zinc. Method, apparatus, and preliminary experiments. J. Res. Natl. Bur. Stand. (U.S.). 79A(6): 737-745; 1975 November-December.

[24] Koch, W. F.; Diehl, H. Additional results on the value of the Faraday. Talanta 23(7), 509-512; 1976 July.